

Design Guide: TIDA-060032

外部フィールド保護機能付き、非接触型、ホール効果、可変速度トリガの外部フィールド保護機能付きリファレンス・デザイン



概要

このリファレンス・デザインは、ホール効果センサを使用し、トリガ（人間が操作するスイッチ）を実装しています。トリガを押すような動作をすると、その距離に応じて変化する電圧が出力されます。これらのタイプのトリガは、コードレス電動工具、またはトリガ変位情報を利用するその他の最終装置での使用に最適です。この設計は非接触型のアプローチを採用しているため、従来の機械式トリガに比べると摩耗や損傷が減少し、製品寿命を延長できます。低消費電力のホール効果スイッチとロード・スイッチを組み合わせ使用し、トリガを押すような動作が発生していないときは、システムを低消費電力のスタンバイ・モードのまま維持します。さらに、オプションの磁界保護機能も使用できます。この機能は、強力な外部磁界が存在するときは、電圧出力をディスエーブルにします。

リソース


TIDA-060032	デザイン・フォルダ
ホール・トリガ評価基板	ツール・フォルダ
DRV5056 、 DRV5032	プロダクト・フォルダ
TPS709 、 TPS22917	プロダクト・フォルダ
SN74HCS00 、 SN74AUP1G00	プロダクト・フォルダ
TLV9061	プロダクト・フォルダ

特長

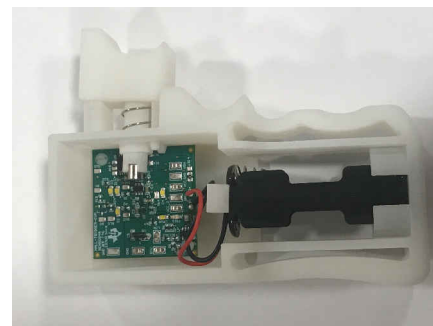
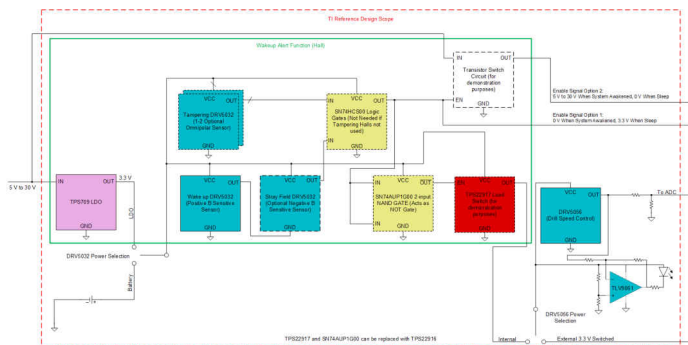
- 最大 10mm のトリガ変位を電圧に変換
 - キャリブレーションなしで測定された電圧誤差: 3% 未満
 - キャリブレーションありで測定された電圧誤差: 0.5% 未満
- (オプション) 強力な外部磁界を検出したときは、電圧出力をディスエーブル化
- 単四電池または 5~30V の外部電源電圧で動作
- スリープ・モードでのシステム消費電流の低減
 - 選択した外部の磁界に対する最大保護: 6.9μA
 - 選択した外部の磁界に対する最小保護: 3.5μA

アプリケーション

- コードレス電動工具
- 外科用機器
- ミキサー、ブレンダー、フード・プロセッサ
- 商用電源で動作する電動工具



テキサス・インスツルメンツの TI E2E™ サポート・エキスパートにお問い合わせください。



1 System Description

Many end equipment require user-provided position information to properly function. From a user's perspective, the inputs can be provided by various methods, such as pressing a button, pressing a trigger, or turning a knob. A mechanism is often needed to translate the inputs from the user to a form that can be sensed and then acted on by the electronics within the system. As an example, cordless power tools like power drills require a mechanism to translate the trigger displacement into a voltage that controls the speed of the tool. Potentiometers are commonly used for translating how far the user presses the trigger into an output voltage, however, this type of mechanical implementation has issues with wear and tear that reduce product lifetime.

To reduce current consumption, cordless power drills are also put in a low-power mode to prevent from draining the battery of the tool. Pressing the trigger wakes up the power drill. Mechanical implementations such as mechanical switches may be used to wake up the system once the trigger displacement exceeds a minimum threshold distance. Mechanical switches also have issues with wear and tear, similar to potentiometers.

In this reference design, a contactless trigger is implemented using Hall-effect sensors, which reduces wear and tear compared to traditional triggers that use potentiometers and mechanical switches. This design includes a 3D-printed trigger module with embedded magnet for illustrating a Hall-based trigger press mechanism. In this implementation, a magnet is placed so that it moves along with the trigger. As the trigger is pressed, the magnet approaches a linear Hall sensor, which translates the sensed magnetic flux density from the moving magnet into an output voltage. Since the sensed magnetic flux density and output voltage varies with the location between the magnet and the linear Hall sensor, the output voltage provides information on the location of the magnet, and therefore, the trigger displacement. This design translates up to 10 mm of trigger displacement into an output voltage.

A load switch is used to disconnect power to the linear Hall sensor and other components if the trigger is not pressed. To wake up the system to enter active mode, the design utilizes a Hall-effect switch for detecting when the trigger displacement exceeds the turn-on distance. When the sensed magnetic flux density of the wake-up Hall-effect switch exceeds the magnetic operating point (B_{OP}) of the switch, the output of the Hall-effect switch is asserted low, which triggers the load switch to reconnect power to the linear Hall sensor.

In addition to the wake-up Hall-effect switch, additional Hall-effect switches are present for implementing optional protection against external magnetic fields. If these additional Hall-effect switches detect strong external magnetic fields, the output of the linear Hall-sensor is disabled by disconnecting power to it, thereby preventing the power drill from accidentally turning ON due to strong external magnetic fields tampering with the system. This protection also turns OFF a currently ON drill when strong magnetic fields are present. Each of the tamper Hall sensors can be individually disabled, which enables the user to select the number of Hall sensors needed for their system based on their sleep current consumption, and external magnetic field protection requirements.

This design supports standalone operation or connection to external systems for in-system evaluation. In standalone operation, the design is powered from AAA batteries that are inserted into the battery holder that comes with the HALL-TRIGGER-EVM. To illustrate status, the following LEDs are used:

- LEDs on the output of each Hall-effect switch
- An LED added to the VCC input of the linear Hall sensor for indicating system wake up from its sleep mode and when the linear Hall sensor is powered
- An LED that changes its brightness based on how far the trigger is pressed

For connecting to external systems for in-system evaluation, an LDO is included in the design to convert external battery voltages from 5 V to 30 V down to a 3.3-V rail that powers the design. Instead of connecting the DRV5056 power to the load switch output, the design can also be reconfigured so that the DRV5056 is powered from an external 3.3-V rail. In addition, an optional BJT circuit on the design is present (this is not populated by default) to translate the internally generated 3.3-V system wake-up signal to a voltage set to the voltage of the external battery.

In addition to being applicable to cordless power tools, this design is also applicable for other end equipment that have a trigger mechanism, such as surgical equipment, mains powered tools, and food blenders.

1.1 Key System Specifications

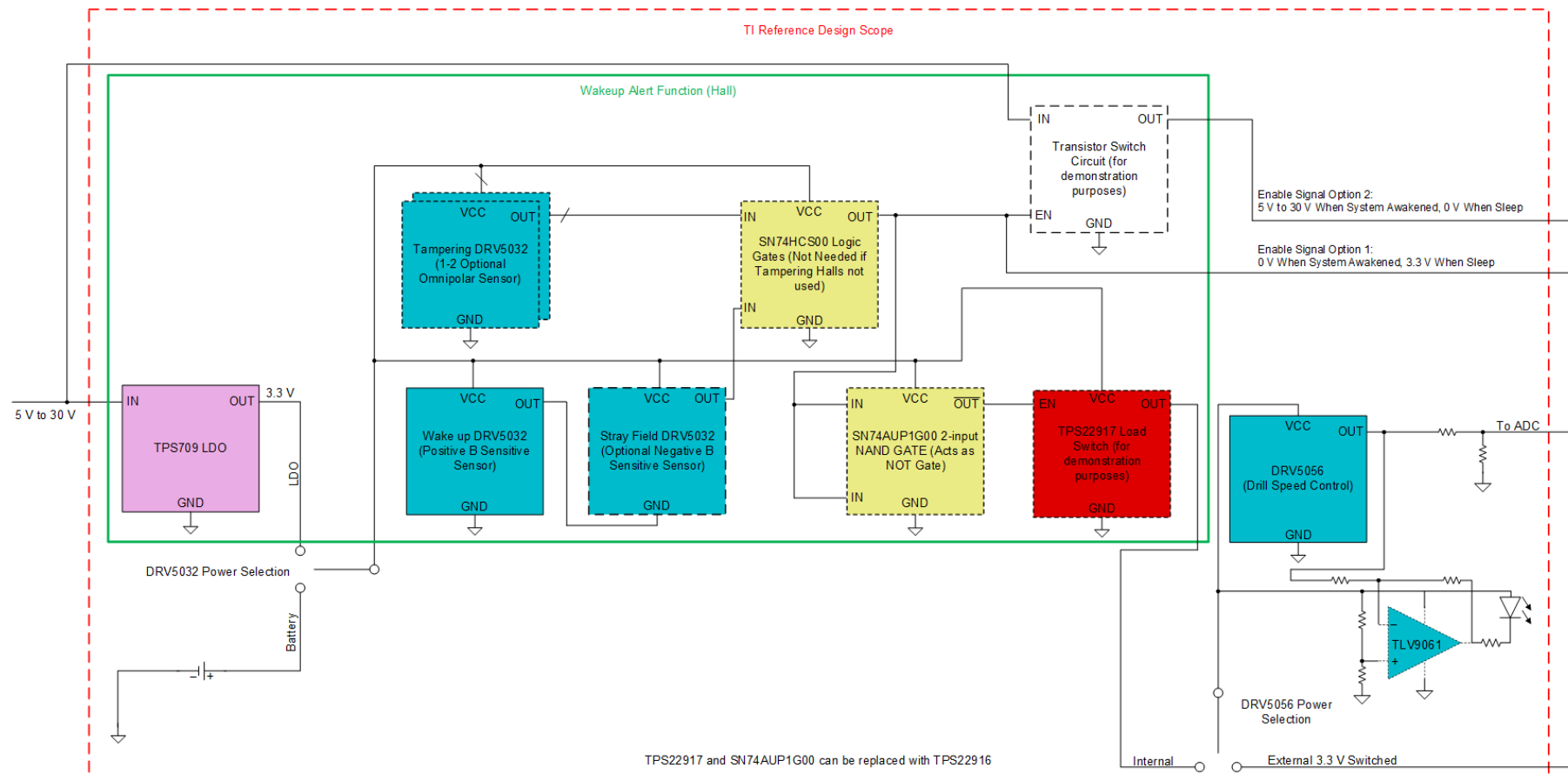
表 1-1. Key System Specifications

FEATURES	DESCRIPTION
Maximum trigger displacement distance	<p style="text-align: center;">Note</p> <p>The actual maximum trigger distance observed with the HALL-TRIGGER-EVM is less than this due to the force from the spring preventing the 10-mm displacement from being observed.</p>
Magnet Specs	<ul style="list-style-type: none"> • Dimensions: 3/16 in diameter (4.7625 mm) × 3/16 in thick (4.7625 mm) • Material: NdFeB, Grade N52 • Magnetization Direction: Axial (Poles on Flat Ends) • Link to Magnet: https://www.kjmagnetics.com/proddetail.asp?prod=D33-N52
Voltage output range	0.9 V to 3.1 V
Measured Voltage output accuracy (without calibration)	< 3%
Measured Voltage output accuracy (with calibration)	< 0.5%
Power Supply Options	<ul style="list-style-type: none"> • Option 1: 2 AAA batteries • Option 2: External 5 V to 30 V on LDO input
Time needed to exit sleep mode and enter active mode	<ul style="list-style-type: none"> • 50 ms if stray field Hall-effect switch disabled • 100 ms if stray field Hall-effect switch enabled
Response time of tamper Hall-effect switches	50 ms
Sleep mode current consumption	<ul style="list-style-type: none"> • 18 V at LDO input, all Hall-effect switches enabled: 7 μA • 18 V at LDO input, one tamper Hall-effect switch disabled: 5.2 μA • 18 V at LDO input, two tamper Hall-effect switches disabled: 3.4 μA • 18 V at LDO input, two tamper Hall-effect switches disabled, stray-field Hall-effect switch disabled: 3.4 μA • LDO disabled, 3.3 V applied directly to VCC, two tamper Hall-effect switches disabled, stray-field Hall-effect switch disabled: 1.7 μA

2 System Overview

2.1 Block Diagram

2-1 depicts the block diagram of this reference design.



2-1. TIDA-060032 Block Diagram

This design is powered from either two AAA batteries (default configuration) or an external 5-V to 30-V power supply. To translate the external power supply voltage to the 3.3-V rail utilized by the reference design, the TPS709 LDO is used. This ultra-low quiescent current, low-dropout (LDO) linear regulator allows the design to be powered from the higher voltage batteries typically seen in cordless power drills.

When the trigger is pressed, a magnet attached to the trigger moves along it. The magnet selected is a 3/16 in × 3/16 in cylinder magnet made of neodymium grade 52. The DRV5056 translates the sensed magnetic flux density from this magnet into an output voltage. When interfacing to an external power drill, this output voltage can be connected to the ADC of an integrated motor driver or microcontroller for changing the speed of the drill. The design has resistor dividers to scale the output voltage from the DRV5056 to a voltage input range suited for the ADC.

To maximize battery lifetime, the design is placed in a sleep mode until a wake-up event by pressing the trigger. A wake-up DRV5032 Hall-effect switch detects when the trigger is pressed by measuring the magnetic flux density of the trigger magnet. The DRV5032 device variant selected for the wake-up sensor is a unipolar sensor that responds to positive magnetic flux density readings. When the trigger is pressed, the sensed magnetic flux density at this Hall-effect switch is greater than the magnetic operating point (B_{OP}), resulting in the output of the DRV5032 to be asserted low and the design to be awakened from sleep mode into active mode. The magnetic flux density at this sensor drops below the switch release point (B_{RP}) when the trigger returns back to its original position, resulting in the output of the DRV5032 to be asserted high and the design to be placed back in sleep mode. Since this sensor must always be ON, it is powered directly from VCC.

The output of the wake-up Hall-effect sensor can be falsely triggered to be asserted low when exposed to a positive magnetic flux from a strong magnet that is external to the system. This external magnet is not to be confused with the trigger magnet, which is internal to the system. The design has three optional, additional DRV5032 devices to prevent the system from entering active mode in the presence of external magnetic fields, even if the wake-up Hall sensor is falsely triggered to be asserted low by the external magnetic fields. Each of these three additional Hall sensors can be individually disabled, which allows selection of the desired level of protection against external magnetic fields.

One of the additional DRV5032 devices is referred to as the stray field sensor. The stray field sensor is a unipolar sensor that responds to the negative magnetic flux. To reduce current consumption, the stray field sensor is only powered when the wake-up Hall sensor is asserted low, which occurs when the trigger is pressed or if the wake-up Hall sensor detects a strong, positive magnetic flux density reading. During the entire 10-mm trigger displacement path, the stray field sensor should detect negative magnetic flux density readings from the trigger magnet and the sensed magnetic flux density of the stray field sensor should exceed the absolute value of the B_{OP} of that sensor. Regardless of the state of the wake-up or other Hall sensors, the system is in sleep mode if the stray field sensor detects positive magnetic flux density readings or if the absolute value of the sensed magnetic flux density does not exceed the absolute value of B_{OP} . As a result, if a strong external magnet is applied to this design and it causes the stray field sensor to detect a net positive magnetic flux density reading, the system will still be placed in sleep mode even if the output of the wake-up Hall sensor is falsely triggered to be asserted low, thereby helping to prevent the design from turning ON due to the wake-up Hall sensor being accidentally triggered by external magnets.

Even with the stray field sensor, it is possible to fool the design into waking up from sleep mode using a strong, external magnet if the external magnet causes the wake-up sensor to detect a positive magnetic flux density while the stray field sensor detects a negative magnetic flux density. To make this design robust to this scenario, two other optional DRV5032 sensors can be used in this design. These other DRV5032 devices are referred to as the tamper Hall-effect sensors and are powered from VCC. The tamper Hall sensor variants used in this design are omnipolar devices that respond to both positive and negative magnetic flux density readings. Regardless of the state of the other Hall sensors, the system is put in sleep mode if any of the two tamper Hall sensors detects a strong, external magnetic field.

When any of the tamper sensors are enabled, a logic gate is needed to combine the outputs from the different Hall sensors to produce one signal that informs the design when the system should be in sleep mode or active mode. The SN74HCS00 quadruple 2-input NAND gate combines the outputs from the different Hall sensors to produce an active-low signal that is asserted low when the system should be awake and asserted high when the system should be in sleep mode. If tamper Hall sensors are not needed, the reference design can be redesigned

to not use the SN74HCS00 by using the following signals as the active-low wake-up signal instead of the SN74HCS00 output:

- The output stray field's Hall-effect switch's output if the stray field sensor is not needed
- The wake-up Hall-effect switch if the stray field is also not enabled.

The TPS22917 in this design is a load switch that can disconnect power from the DRV5056 when the system is asleep, thereby reducing current consumption. Since the TPS22917 has an active high switch control input and the SN74HCS00 produces an active low input, the output from the SN74HCS00 must be inverted before connecting to the switch control input of the TPS22917. The SN74AUP1G00 single 2-input NAND gate is configured to do this signal inversion. Note that the design can also be redesigned to replace the active-high TPS22917 and SN74AUP1G00 with just one active-low TPS22916 device.

As an alternative to powering the DRV5056 from the output of the TPS22917, the DRV5056 in this design can also be powered from a voltage-regulated, external 3.3-V power supply. If reducing the current consumption is desired, the power to the DRV5056 can be switched OFF externally when the system is in sleep mode.

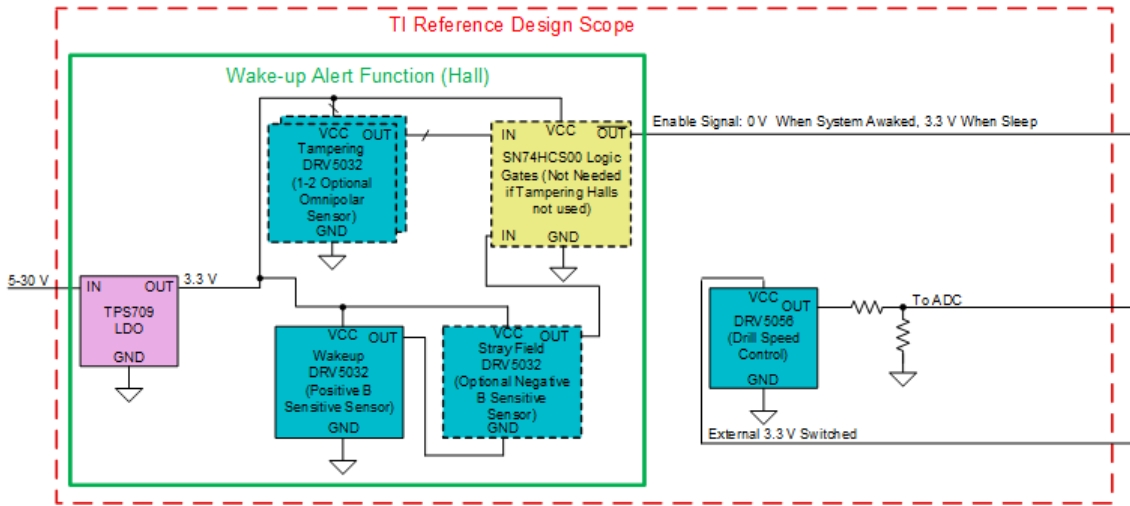
In addition, there are two enable signal options in the design that can be used to provide information to any external systems about whether the design is in sleep mode or active mode. The first enable signal comes from the output of the SN74HCS00. This enable signal is at 0 V when the design is in sleep mode up and 3.3 V when in active mode. For external signals that require an enable signal with a higher voltage, select the second enable signal option.

The second enable option is created by taking the first enable signal and feeding it into an NPN transistor switch circuit. Connect the voltage source input to the NPN circuit to a drill battery to produce a wake-up signal that is at the voltage level of the drill. As an example, if the voltage input of the circuit is connected to an 18-V drill battery, the second enable option will have an output voltage of 18 V when the system is in active mode and 0 V when the system is asleep (note that this is the opposite polarity of enable signal option 1). If enable signal option 2 is not needed, remove the NPN transistor circuit from the design. By default, the NPN transistor circuit is not populated on the design.

An example use-case for the enable signals is for triggering any external systems connected to the design to go to sleep or active mode along with the design. To trigger the external systems for sleep mode, one option is to remove power from these external systems using an external eFuse, load switch, or hot swap controller that has an enable pin that connects to one of the enable signals from this design. Based on the voltage generated by the enable signal of the design, the power to the external system is either connected or disconnected accordingly.

The design also has a TLV9061 op amp; however, this op amp is just for driving one of the LEDs to change its brightness based on the output voltage of the DRV5056. This LED is for showcasing the movement of the trigger when the design is in standalone mode. Since it is mainly for demonstration purposes, this circuit is not needed in final system implementations.

Note that this design has components that were added to demonstrate this design in a standalone mode. [Figure 2-2](#) shows a simplified version of this block diagram that excludes the components in the design that are for showcasing standalone mode, so they are not needed in a final system implementation. In the simplified block diagram, it assumes that there is an external device that turns OFF power to the system based on the output enable signal and that the DRV5056 is powered from an external power supply that is automatically disabled when the system is in sleep mode. In addition, if protection against external magnetic fields is not needed, the tamper DRV5032, stray field DRV5032, and SN74HCS00 can be removed from this simplified block diagram.



2-2. Block Diagram With Demonstration Components Removed

2.2 Highlighted Products

2.2.1 DRV5056

The DRV5056 is a linear Hall-effect sensor that responds proportionally to positive magnetic flux density readings. The device uses a ratiometric architecture that can reduce error from VCC tolerance when the external analog-to-digital converter (ADC) uses the same VCC for its reference. The DRV5056 is sensitive to the magnetic field component that is perpendicular to the die inside the package. [Figure 2-3](#) shows the direction of sensitivity for the DRV5056.

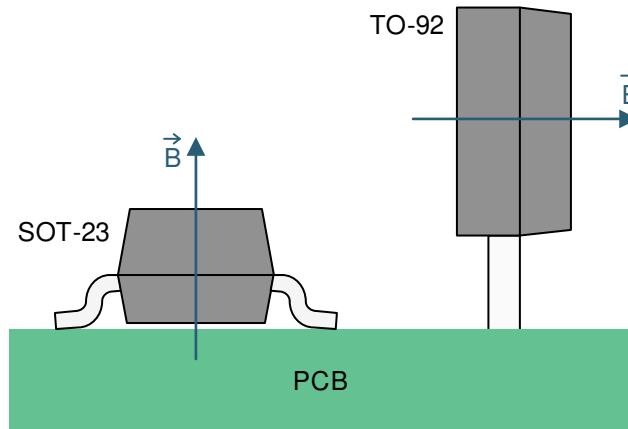


Figure 2-3. DRV5056 Direction of Sensitivity

This design uses the TO-92 through-hole package. For the TO-92 package of this device, a positive magnetic flux density is defined as when the magnetic south pole applied near the front (marked) of the package or a north pole applied from behind the package. [Figure 2-4](#) shows the magnetic response of the device. This device is a unipolar device, where the analog output drives 0.6 V when no magnetic field is present and increases as the positive field becomes stronger.

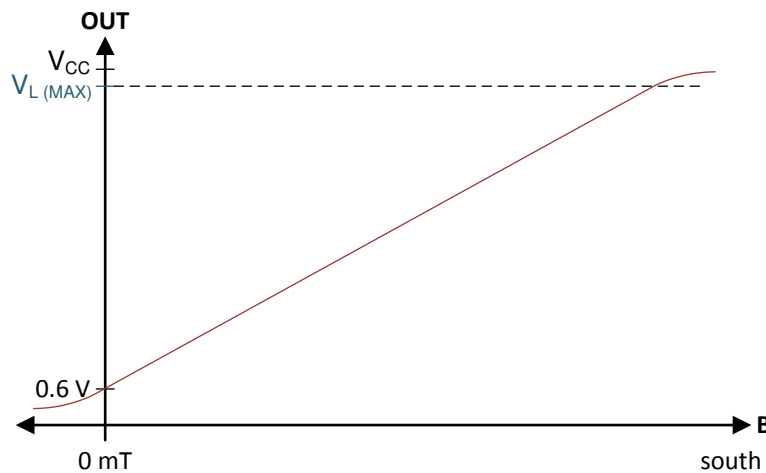


Figure 2-4. DRV5056 Magnetic Response

The bipolar DRV5055 can be used as an alternative to the DRV5056. The DRV5055 responds to both positive and negative fields instead of just negative fields. The advantage of the DRV5055 is that it can still work if the magnet was accidentally installed backwards since the device senses both negative and positive fields (note that the wake-up and stray field sensors will not work if the magnets are reversed because they are unipolar as well). For the [head-on configuration](#) used in this design, the linear Hall sensor is only exposed to either a positive field or a negative field during the trigger movement; it is not exposed to both fields when the trigger is pressed. For more information, see the [Head-on Linear Displacement Sensing Using Hall-Effect Sensors](#) application brief. As a result, only half the range of the DRV5055 is used if the DRV5055 is used as the linear Hall sensor for the

design. Since the DRV5056 is a unipolar device; however, the entire range of the DRV5056 can be used. To maximize output dynamic range, the DRV5056 was selected in this design instead of the DRV5055.

The DRV5056A1 device variant was selected in this design because its magnetic range (20 mT) is near the maximum magnetic flux density that is expected to be detected by the DRV5056 based on the magnet material, magnet dimensions, and the distance from the magnet to the DRV5056 sensing element.

2.2.2 DRV5032

The DRV5032 device is an ultra-low-power digital switch Hall-effect sensor, designed for the most compact and battery-sensitive systems. The device is offered in multiple magnetic thresholds, sampling rates, output drivers, and packages to accommodate various applications. 表 2-1 (from the data sheet) shows a comparison between the different DRV5032 device variants.

表 2-1. DRV5032 Device Variants

VERSION	MAXIMUM THRESHOLD	MAGNETIC RESPONSE	OUTPUT TYPE	SAMPLING RATE	PACKAGES AVAILABLE
DRV5032DU	3.9 mT	Unipolar	Push-pull	20 Hz	SOT-23, X2SON, TO-92
DRV5032FA	4.8 mT	Omnipolar	Push-pull	20 Hz	SOT-23, X2SON, TO-92
DRV5032FB		Omnipolar	Push-pull	5 Hz	SOT-23, TO-92
DRV5032FC		Omnipolar	Open-drain	20 Hz	SOT-23, TO-92
DRV5032FD		Unipolar	Push-pull	20 Hz	X2SON, TO-92
DRV5032AJ		9.5 mT	Omnipolar	Open-drain	20 Hz
DRV5032ZE	63 mT	Omnipolar	Open-drain	20 Hz	SOT-23, TO-92

図 2-5 shows the direction of sensitivity for the different DRV5032 device variants. When the applied magnetic flux density exceeds the B_{OP} threshold, the device outputs a low voltage. The output stays low until the flux density decreases to less than B_{RP} , and then the output either drives a high voltage or becomes high impedance, depending on the device version. By incorporating an internal oscillator, the device samples the magnetic field and updates the output at a rate of 20 Hz, or 5 Hz for the lowest current consumption. Omnipolar and unipolar magnetic responses are available.

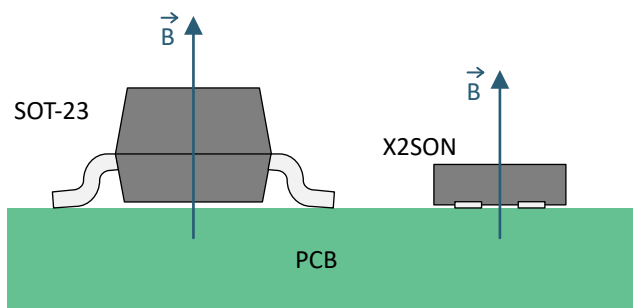


図 2-5. DRV5032 Direction of Sensitivity

In the design, the X2SON package of the DRV5032DU is used for the wake-up (U1) and stray field sensors (U2). This device variant is selected for both of these sensors because it was unipolar and had both a positive-responding and negative-responding output. In addition, the 3.9-mT B_{OP} threshold works well for the selected magnet and magnet to sensor distances used in this design.

The SOT-23 package of the DRV5032FA is selected for the U3 and U4 tamper switches. This device is selected for the following reasons:

- It is omnipolar, which means it could respond to both a strong positive and a strong negative field from external magnets
- It uses a push-pull output, which consumes less current than an open-drain output type
- The 4.8-mT B_{OP} threshold works well for the selected magnet and magnet-to-sensor distances used in this design

- The 20-Hz sampling rate allows detecting external magnetic fields in 50 ms compared to the 200-ms detection rate if a 5-Hz device variant is selected. If the system can use a 200-ms detection rate, the DRV5032FA in this design can be replaced with a DRV5032FB to reduce system current consumption.

2.2.3 TPS709

The TPS70933 linear regulator is an ultra-low quiescent current devices designed for power-sensitive applications. The device can take an input voltage of up to 30 V, which allows it to regulate the high voltage from many cordless power tool batteries into a 3.3-V rail. A precision band-gap and error amplifier provides 2% accuracy over temperature. A quiescent current of only 1 μ A makes these devices ideal solutions for battery-powered, always-on systems that require very little idle-state power dissipation. These devices have thermal-shutdown, current-limit, and reverse-current protections for added safety.

The TPS70933 device is used in this design to power the DRV5032 from the relatively higher-voltage batteries that are in cordless power tools. This device was chosen for this design because of its low current consumption, high input voltage, and its 3.3-V output voltage. For systems with more relaxed current consumption and input voltage requirements, the TLV70433 is an alternative LDO that could also be used for a lower cost system.

2.2.4 SN74HCS00

The SN74HCS00 contains four independent 2-input NAND gates with Schmitt-trigger inputs. Each gate performs the Boolean function: $\overline{Y} = \overline{A \times B}$. The device has a wide operating voltage range of 2 V to 6 V and has a typical supply current of 100 nA. The SN74HCS00 is used to combine the outputs from the different Hall switches to produce one output that tells the system when it should be in sleep or active mode. This specific device was selected because of its low current consumption and cost.

2.2.5 TPS22917

The TPS22917 device is a small, single-channel load switch utilizing a low leakage P-channel MOSFET for minimum power loss. The switch ON state is controlled by a digital switch control input that can interface directly with low-voltage control signals. The device has an input voltage range of 1 V to 5.5 V and has a 10-nA current consumption when it is in its OFF state. The switch control input is active high. If a high voltage is applied to the switch control input, the load switch is in the ON state and the VOUT pin is connected to the VIN pin of the device. On the other hand, if a low voltage is applied to the switch control input, the load switch is in the OFF state and the VOUT pin is disconnected from the VIN pin of the device.

In this design, the TPS22917 is used to disconnect the power supply of the board (connected to VIN of the TPS22917) from the VCC pin of the DRV5056 (connected to VOUT of the TPS22917). When the system is in sleep mode, the TPS22917 disconnects VCC from the DRV5056, thereby reducing system current consumption. The TPS22917 was selected because of its cost and its low OFF-state current consumption. The active-high TPS22917 and the SN75AUP1G00 can be replaced with one active-low TPS22916.

2.2.6 SN74AUP1G00

The SN74AUP1G00 contains one 2-input NAND gate that performs the Boolean function: $\overline{Y} = \overline{A \times B}$. The device has an operating voltage range of 0.8 V to 3.6 V and has a maximum supply current of 900 nA. The SN74AUP1G00 is used to convert the active high switch control input of the TPS22917 to an active-low switch control input. This device was selected because of its low cost, low current consumption, and its support of 3.3-V logic. The active-high TPS22917 and the SN75AUP1G00 can be replaced with one active-low TPS22916.

2.2.7 TLV9061

The TLV9061 is a single low-voltage op amp with rail-to-rail input- and output-swing capabilities. This device translates the DRV5056 voltage into a voltage that changes the brightness of an LED on the board based on how far the trigger is pressed. The device was selected because of its low cost. Since this device is mainly used for demonstrating the trigger movement with the LED, note that it is not actually needed in a final implementation of a cordless power tool.

2.3 Design Considerations

2.3.1 Design Hardware Implementation

2.3.1.1 Hall-Effect Switches

Figure 2-6 shows a snippet of the Hall-effect switch portion of the design, where the parts that are labeled U1, U2, U3, and U4 are the Hall-effect switches. In the design, U1 is the primary switch for waking the system up when the trigger is pressed, U2 is the stray field sensor, and U3 and U4 are the tamper Hall sensors.

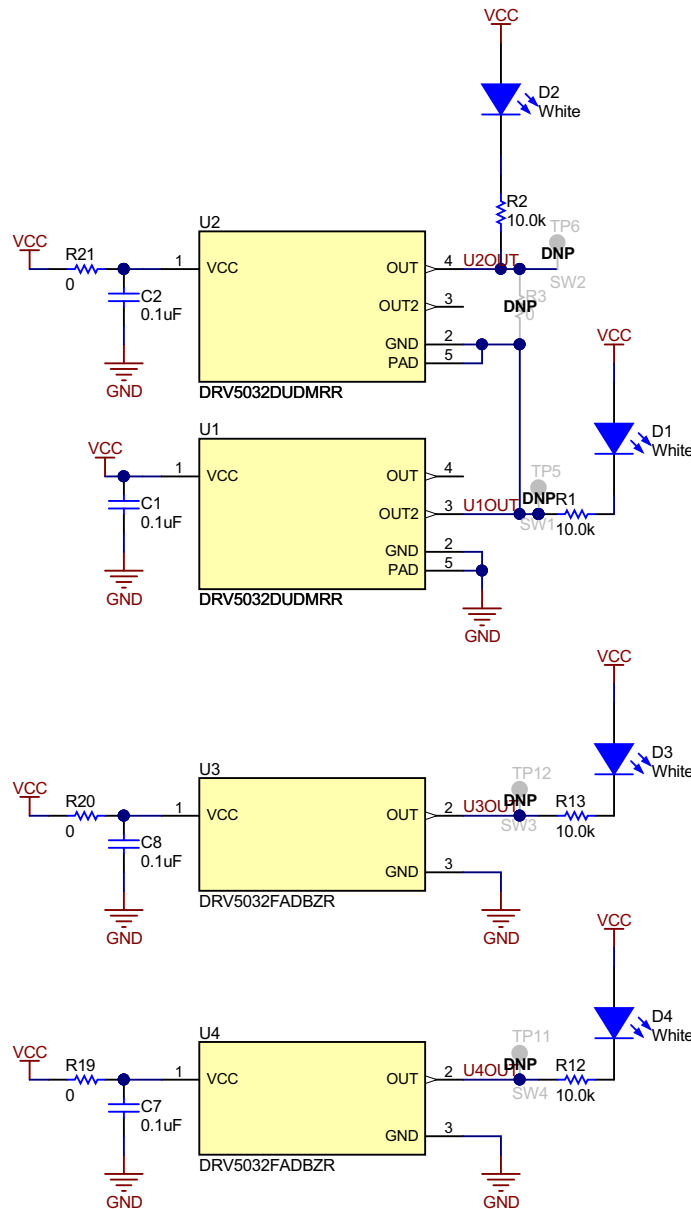


Figure 2-6. Schematic Snippet of Hall-Effect Switch Portion of Design

The DRV5032 is used for each of the four Hall-effect switches in the design. All four of these switches have a 20-Hz sampling rate, a push-pull output type, a test point on the board for probing the switch output, and an LED on the board for visually indicating the status of each switch. Table 2-2 shows how the configurations of the different Hall switches vary in this design.

表 2-2. Configurations of Hall Switches U1–U4

BOARD DESIGNATOR	PURPOSE	DEVICE VERSION	THRESHOLD VALUES	MAGNETIC RESPONSE	PACKAGE	POWER STATE
U1	Wake-up sensor	DRV5032DU	Output asserted low if $B > 3.9$ mT. Output asserted high if $B < -0.9$ mT.	Unipolar: Responds to south (positive) pole of magnet (OUT2 pin of device is used) applied near top of package	X2SON	Always powered and enabled
U2	Stray-field sensor	DRV5032DU	Output asserted low if $B < -3.9$ mT. Output asserted high if $B > -0.9$ mT.	Unipolar: Responds to north (negative) pole of magnet (OUT pin of device is used) applied near top of the package.	X2SON	Powered when resistor R21 populated and the OUT2 pin of U1 is asserted low
U3	Tamper sensor 1	DRV5032FA	Output asserted low if $ B > 4.8$ mT. Output asserted high if $ B < 0.5$ mT.	Omnipolar: responds to north and south poles of magnet applied near top of package.	SOT-23	Always powered if resistor R20 populated
U4	Tamper sensor 2	DRV5032FA	Output asserted low if $ B > 4.8$ mT. Output asserted high if $ B < 0.5$ mT.	Omnipolar: responds to north and south poles of magnet applied near top of package.	SOT-23	Always powered if resistor R19 populated

For the DRV5032, a negative field is defined as when the north pole of a magnet is applied near the top of the package containing the device, as shown in 図 2-7. A negative field is also detected when the south pole of a magnet is applied underneath the bottom of the package that has the device. A positive field is defined as when the south pole of a magnet is applied near the top of the package or when the north pole of a magnet is applied underneath the bottom of the package containing the device.

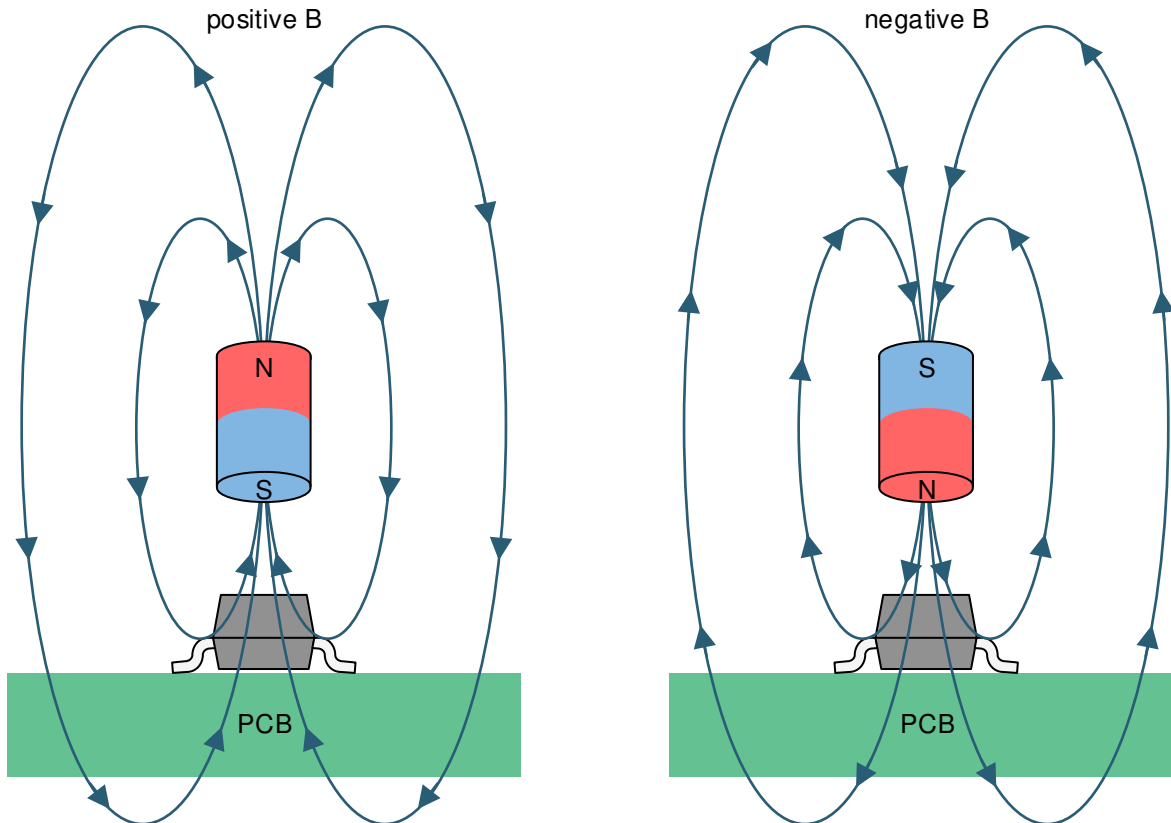


図 2-7. Flux Direction Polarity

In the design, the 4-pin X2SON package of the DRV5032DU device variant is used for devices U1 and U2. This device variant is a dual output unipolar device, where each output only responds to either a positive field or a negative field. 図 2-8 shows the output waveforms of the DRV5032DU device variant.

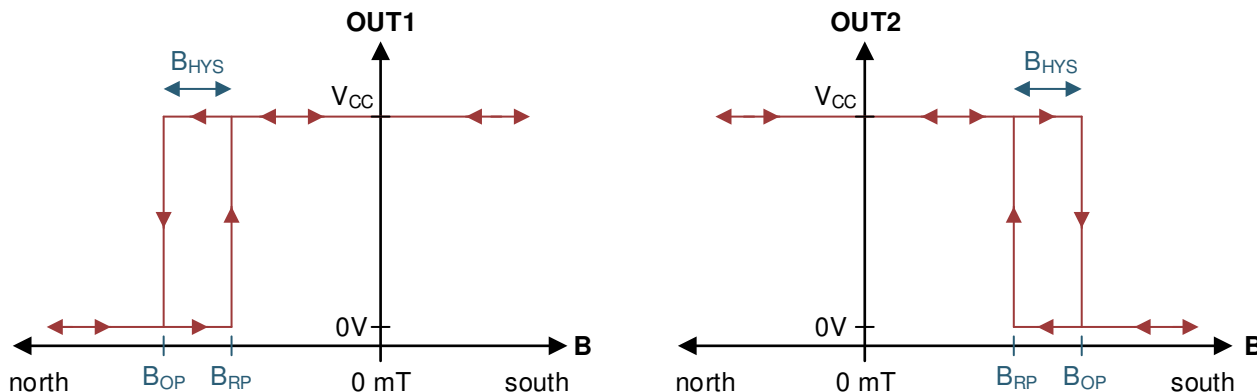


Figure 2-8. DRV5032DU Output Waveforms

The OUT1 pin of the U1 and U2 devices (referred to as the OUT pin in Figure 2-7) only responds to negative magnetic flux density readings. This output is not affected by positive magnetic flux density readings. Figure 2-9 shows the data sheet spec for the B_{OP} and B_{RP} range of the OUT1 output. If the sensed magnetic flux density is less than the B_{OP} spec of the OUT1 output of the DRV5032DU device variant, the OUT1 output will be asserted low. If the sensed magnetic flux density is greater than the B_{RP} spec of the OUT1 output of the DRV5032DU device variant, the output will be asserted high. Based on the B_{OP,MIN} and B_{RP,MAX} range of the OUT1 Hall sensor, the OUT1 output is assured to be asserted low when the sensed magnetic flux density is less than -3.9 mT and asserted high when the sensed magnetic flux density is greater than -0.9 mT.

The OUT2 pin of the U1 and U2 devices, on the other hand, only responds to positive magnetic flux density readings. Figure 2-9 shows the data sheet spec for the B_{OP} and B_{RP} range of the OUT2 output. If the sensed magnetic flux density is greater than the B_{OP} spec of the OUT2 output of the DRV5032DU device variant, the OUT2 output will be asserted low. If the sensed magnetic flux density is less than the B_{RP} spec of the OUT2 output of the DRV5032DU device variant, the output will be asserted high. Based on the B_{OP,MIN} and B_{RP,MAX} range of the OUT2 Hall sensor, the OUT2 output is assured to be asserted low when the sensed magnetic flux density is greater than +3.9 mT and asserted high when the sensed magnetic flux density is less than +0.9 mT.

PARAMETER	TEST CONDITIONS	MIN	TYP	MAX	UNIT	
DU VERSION						
B _{OP}	Magnetic threshold operate point	OUT1 pin (north) ⁽²⁾	-3.9	-2.5	-1.2	mT
		OUT2 pin (south)	1.2	2.5	3.9	
B _{RP}	Magnetic threshold release point	OUT1 pin (north) ⁽²⁾	-3.5	-1.8	-0.9	mT
		OUT2 pin (south)	0.9	1.8	3.5	
B _{HYS}	Magnetic hysteresis: B _{OP} - B _{RP}	Each output	0.1	0.7	1.9	mT
FA, FB, FC VERSIONS						
B _{OP}	Magnetic threshold operate point		±1.5	±3	±4.8	mT
B _{RP}	Magnetic threshold release point		±0.5	±1.5	±3	mT
B _{HYS}	Magnetic hysteresis: B _{OP} - B _{RP}		0.8	1.5	3	mT

Figure 2-9. B_{OP} and B_{RP} Range of DRV5032DU and DRV5032FA Outputs

For devices U3 and U4, the 3-pin SOT-23 package of the DRV5032FA device variant is used. This device is a single output omnipolar device, which responds to both positive and negative magnetic flux density readings the same way. Figure 2-10 shows the output waveform of the DRV5032FA device variant.

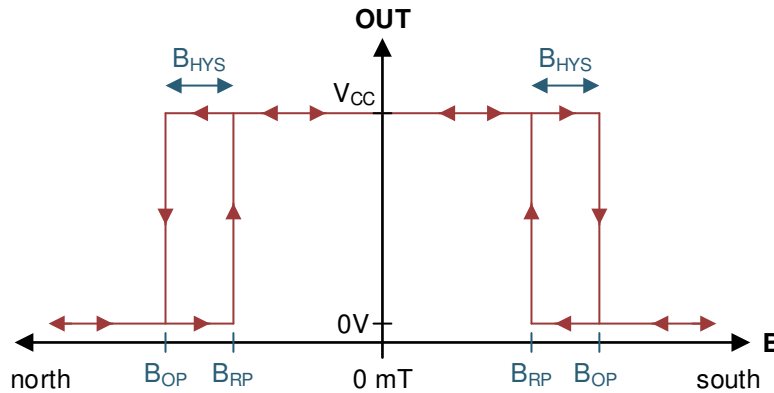


图 2-10. DRV5032FA Output Waveform

The OUT pin of the U3 and U4 devices responds to both negative and positive magnetic flux density readings. 图 2-8 shows the data sheet spec for the B_{OP} and B_{RP} range of this device variant. If the absolute value of the sensed magnetic flux density is greater than the B_{OP} spec of the DRV5032FA, the OUT output will be asserted low. If the absolute value of the sensed magnetic flux density is less than the B_{RP} spec of the DRV5032DU device variant, the output will be asserted high. Based on the B_{OP,MIN} and B_{RP,MAX} range of the Hall sensor, the OUT output is assured to be asserted low when the absolute value of the sensed magnetic flux density is greater than 4.8 mT and asserted high when the absolute value of the sensed magnetic flux density is less than 0.5 mT.

2.3.1.1.1 U1 Wake-Up Sensor Configuration

The primary function of the U1 switch is to keep the system in low power when the trigger is not pressed. This switch is always powered and enabled. U1 uses the OUT2 pin of the unipolar DRV5032DU X2SON package, so it only responds to a positive magnetic flux density. OUT2 is assured to be asserted low when the sensed magnetic flux density is greater than +3.9 mT and asserted high when the sensed magnetic flux density is less than +0.9 mT.

The OUT2 pin of U1 is connected to the GND pin of the U2 sensor so that the U2 Hall sensor is only powered when the wake-up sensor detects a positive magnetic flux density from pressing the trigger or if an external magnet causes a positive magnetic flux density reading that triggers U1 into asserting its output low. If no external magnetic field is applied or the trigger is not pressed, U2 is not powered, which reduces the current consumption compared to if U2 was always powered. One disadvantage of connecting the output of one switch to the GND of another switch is that it can increase the response time of the system by the sampling period + power-on time of one Hall sensor (≈ 50 ms in this case). Additionally, note that since the maximum output current supported by the DRV5032 is ± 5 mA and the peak current consumption of the DRV5032 is 2.7 mA, do not connect the output of a Hall sensor to the GNDs of any other Hall sensors. Consequently, switches U3 and U4 do not have their ground connected to the OUT2 pin of U1.

2.3.1.1.2 U2 Stray-Field Sensor Configuration

Switch U2 is the stray field sensor. U2 is an optional sensor that can be disabled by depopulating resistor R21 on the board and placing a 0- Ω resistor between pads 1 and 2 of the R16 3-pad footprint. The GND pin of U2 is connected to the OUT2 output of U1, and is therefore, only powered if the output of U1 is asserted low. Note that because U2 is not powered on when Switch 1 is inactive, its actual voltage varies, but remains near the inactive state (logic high) of the load switch.

In addition, U2 uses the OUT1 pin of the unipolar DRV5032DU X2SON package, so it only responds to a negative magnetic flux density reading. OUT1 is assured to be asserted low when the sensed magnetic flux density is less than -3.9 mT and asserted high when the sensed magnetic flux density is greater than -0.9 mT. With U2 being powered from U1, the U2 output is only assured to be asserted low if the sensed magnetic flux density at U1 is greater than B_{OP} of OUT2 while the sensed magnetic flux density at U2 is less than B_{OP} of OUT1. Consequently, the output of U1 is not needed to determine whether the system should be in sleep mode if the U2 stray field sensor is enabled. In this case, the output of U2 provides enough information on the state of U1 and U2.

Since the wake-up sensor only responds to a positive field and the stray field sensor responds only to a negative field, the design is robust against external magnets placed in the orientation shown in [Figure 2-11](#) and unidirectional stray fields exposed to the design. In this orientation, both the wake-up sensor and stray field sensor either detect a strong negative field or a strong positive field. If a strong negative field is applied to both sensors, switch U2 is not powered and the system is placed in sleep mode. If a strong positive field is applied to both sensors, switch U2 is powered, but the system is still placed sleep mode.

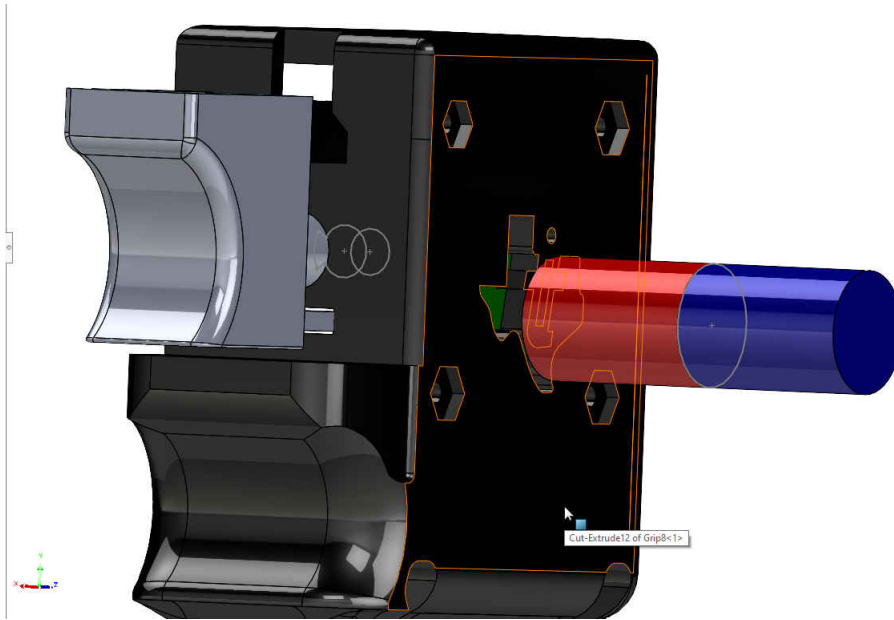


Figure 2-11. External Magnet Orientation Best Detected by Stray Field Sensor

2.3.1.1.3 U3 and U4 Tamper Sensor Configuration

Switches U3 and U4 are the optional tamper sensors. To disable switch U3, depopulate resistor R20 and place a 0-Ω resistor between pads 1 and 2 of the R18 3-pad footprint. Switch U4 can also be disabled by depopulating resistor R19 and placing a 0-Ω resistor between pads 1 and 2 of the R17 3-pad footprint. U3 and U4 have their GND pins connected to the GND of the board instead of an output of a Hall sensor, so they are always powered as long as resistors R19 and R20 are populated. Both of these devices use the DRV5032FA SOT-23 package and respond to both positive and negative magnetic flux density readings. The output of these devices is asserted low when the absolute value of the sensed magnetic flux density is greater than 4.8 mT and asserted high when the absolute value of the sensed magnetic flux density is less than 0.5 mT.

Switches U3 and U4 are for making the design robust against the magnet orientation shown in [Figure 2-12](#). In this orientation, U1 detects a strong positive field and U2 detects a strong negative field, thereby triggering the wake-up sensor and stray field sensor. Switches U3 and U4 can detect the strong magnetic field from this orientation and put the system in sleep mode. These switches are spread out from each other to cover a wider sensing range. U3 and U4 are also placed so that the sensed magnetic flux density from the trigger magnet is small enough to not be misinterpreted as an external magnetic field.

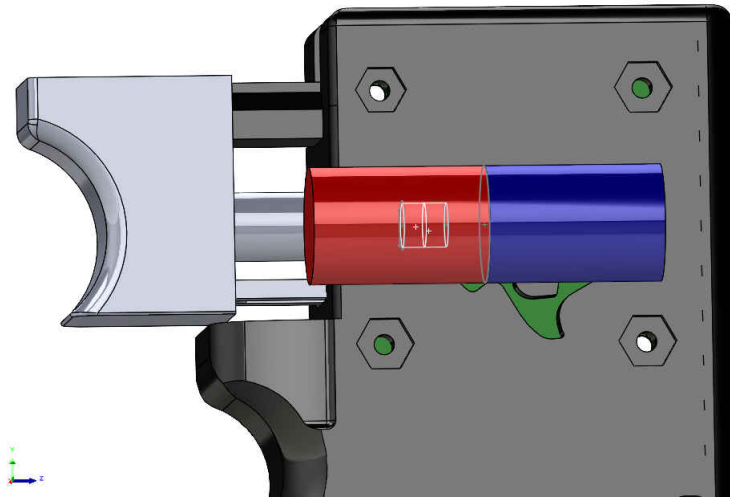


図 2-12. Additional Magnet Orientation Detected by Tamper Hall Sensors

2.3.1.1.4 Hall Switch Placement

The magnetic flux density detected by a Hall sensor is dependent on the magnet dimensions, magnet material, and the distance from the magnet to the sensing element within the Hall sensor. Note that the location of the sensing element varies for each package of the DRV5032. 図 2-13 shows the location of the sensing element in the X2SON and SOT-23 packages of the DRV5032. The two pictures on the right express the sensing location with respect to the bottom of the X2SON and SOT-23 packages of the DRV5032. To express the sensing location so that it is with respect to the top of a package, subtract the readings that are with respect to the bottom of the package from the package height. As an example, if the X2SON package height is 400 μm and the distance from the bottom of the package to the sensing element is 250 μm , the distance from the top of the X2SON package to the sensing element is $400 - 250 = 150 \mu\text{m}$. Similarly, if the SOT-23 height is 1120 μm and the distance from the bottom of the package to the sensing element is 650 μm , the distance from the top of the SOT-23 package to the sensing element is $1120 - 650 = 470 \mu\text{m}$.

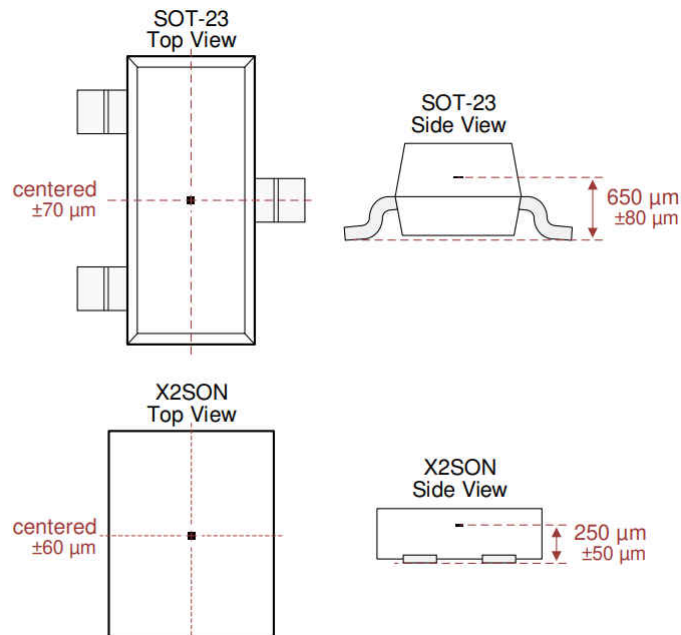


図 2-13. Location of Sensing Element Within X2SON and SOT-23 Packages of DRV5032

Based on the magnet specifications and the distance from the magnet to the sensing elements, simulations were done to estimate the expected sensed magnetic flux density at each sensor across the trigger displacement range. For detailing the distances from the magnet to the Hall sensors, the convention shown in [Figure 2-14](#) was used. In this figure, the z-axis is defined as going from right to left (this is the direction of the trigger movement), the y-axis is defined as going from up to down, and the x direction is defined as going into the page (from the top layer of the PCB to the bottom layer of the PCB).

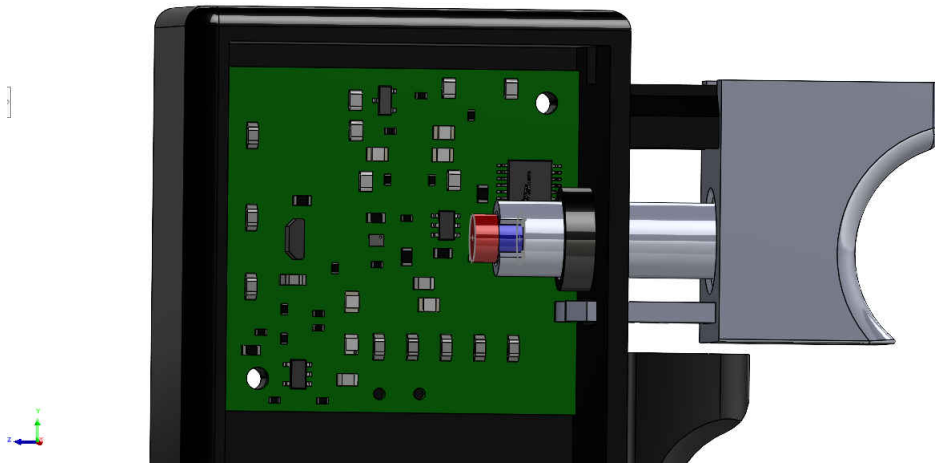


Figure 2-14. Board Picture Within 3D Printed Trigger Module

2.3.1.1.4.1 Placement of U1 and U2 Sensors

The following procedure was used to find the placement of U1 and U2:

1. An initial y-component displacement of 0 mm was selected for switches U1 and U2. In the view shown in [Figure 2-14](#), switch U1 cannot be seen because it is underneath the magnet. [Figure 2-15](#) shows a rotated and zoomed in version of [Figure 2-14](#), which better shows U1. The white dot at the left face of the magnet is the center-point on the surface of the left face of the magnet. Both U1 and U2 are placed so that the sensing element within these devices have no y-direction displacement from the white dot at the magnet.

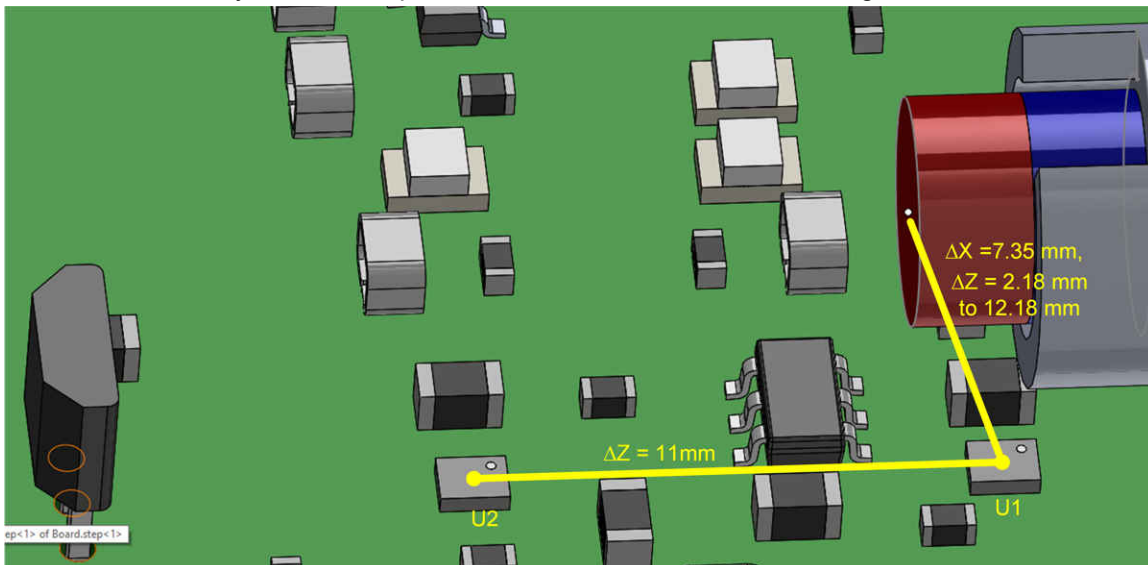


Figure 2-15. Zoomed and Rotated View of Board Within 3D Printed Trigger Module

2. An initial x-component displacement was selected for the distance from the dot on the magnet to U1 and U2. Since U1 and U2 cannot be moved in the x direction due to being surface mount parts with fixed heights, changing the x-component displacement involves moving the magnet in the x direction or putting U1 and U2 on the opposite layer of the PCB. If the magnet is moved in the x direction, note that the impact of this

- change on the DRV5056 output must be verified if the height of the DRV5056 through-hole package cannot be adjusted accordingly.
3. The z-component displacement from U1 to the dot on the magnet was selected. To ensure a more robust design, place U1, which only reacts to a positive field, so that the magnetic field at U1 in the off position is slightly negative. The rest state magnetic field is made slightly negative by slightly displacing U1 in the z direction so that the sensing element is under the north pole of the magnet.
 4. After the z component of U1 was selected, a simulation was done to verify that the sensed magnetic flux density of the sensor was less than B_{RP} when the trigger was at rest. In addition, the sensed magnetic flux density must be greater than B_{OP} for a trigger displacement value of d_{min} to d_{max} , where d_{min} is the desired trigger displacement at which the system is waked up and d_{max} is the largest trigger displacement distance (10 mm for this design). If these conditions are not met, take the following actions:
 - a. Restart from step 3 with a different z-component displacement.
 - b. Restart from step 2 with a different x-component displacement. Note that the impact of this change on the DRV5056 output must be verified if the height of the DRV5056 through-hole package cannot be adjusted accordingly.
 - c. Modify the dimensions or material of the magnet and restart from step 2. Note that the impact of this change on the DRV5056 output must be verified.
 5. The z-component displacement from U2 to the dot on the magnet was selected.
 6. After the z component of U2 was selected, a simulation was done to verify that the sensed magnetic flux density of the sensor was less than B_{OP} during the entire trigger displacement range. If these conditions are not met, take the following actions:
 - a. Restart from step 5 with a different z-component displacement.
 - b. Restart from step 2 with a different x-component displacement. Note that the impact of this change on the DRV5056 output must be verified if the height of the DRV5056 through-hole package cannot be adjusted accordingly.
 - c. Modify the dimensions or material of the magnet and restart from step 2 again. Note that the impact of this change on the DRV5056 output must be verified.

Based on implementing the previous procedures, the following distances were obtained and used for this design:

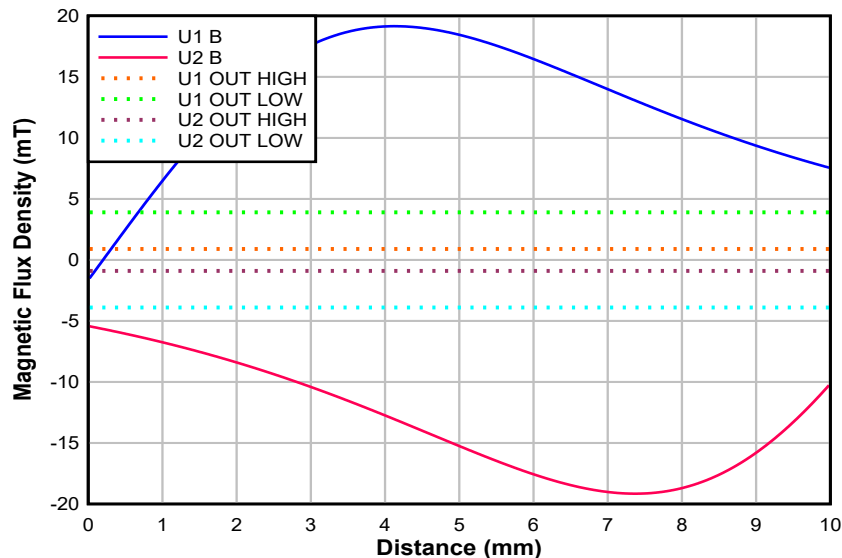
- U1 distance components
 - X-component displacements
 - X-component from top of package to white dot of magnet = 7.35 mm
 - X-component (“sensor z-offset” parameter in tool) from top of package to bottom of magnet = 7.35 – magnet radius = 4.96875
 - X-component (sensor z-offset in tool) from sensing element to bottom of magnet to sensing element = $4.96875 + 0.150 = 5.11875$ mm
 - Y-component displacement = 0 mm
 - Z-component displacement
 - Trigger not pressed
 - Z-component from sensing element to white dot of magnet (d_1 in tool) = 2.18 mm
 - Z-component from sensing element to magnet center = $2.18 - 0.5 \times \text{magnet thickness} = 2.18 - 0.5(4.76) = -0.2$ mm
 - Maximum trigger displacement = 10 mm
 - Z-component from sensing element to white dot of (d_2 in tool) = 12.18 mm
 - Z-component from sensing element to magnet = $12.18 - 0.5 \times \text{magnet thickness} = 12.18 - 0.5(4.76) = 9.8$ mm
- U2 distance components
 - X-component displacement = x-component displacement of U1
 - Y-component displacement = y-component displacement of U1
 - Z-component displacement
 - Z-component displacement from U1 sensing element to U2 sensing element = 11 mm
 - Trigger not pressed
 - Z-component from sensing element to white dot of magnet = -8.82 mm
 - Z-component from sensing element to magnet center = $-8.82 - 0.5 \times \text{magnet thickness} = -8.82 - 0.5(4.76) = -11.2$ mm

- Maximum trigger displacement = 10 mm
 - Z-component from sensing element to white dot of \square 2-15 = 1.18 mm
 - Z-component from sensing element to magnet = 1.18 – 0.5 × magnet thickness) = 1.18 – 0.5(4.76) = –1.2 mm

2.3.1.1.4.1.1 U1 and U2 Magnetic Flux Density Estimation Results

The magnetic flux density detected at switches U1 and U2 were simulated to determine appropriate placement of the Hall-effect sensors. For simulation, the distance measurements are done with respect to the sensing element to the magnet since the simulation tool does not automatically consider the location of the sensing element within the device.

\square 2-16 shows a plot of the simulation results for the U1 and U2 sensors. If the sensed magnetic flux density of U1 is above the U1 OUT LOW horizontal line ($B_{OP,MAX}$) in the results, the output of U1 is assured to be low. If the sensed magnetic flux density of U1 is below the U1 OUT HIGH horizontal line ($B_{RP,MIN}$) in the results, the output of U1 is assured to be high. Similarly, if the sensed magnetic flux density of U2 is below the U2 OUT LOW horizontal line ($B_{OP,MIN}$) in the results and it is powered, the output of U2 is assured to be low. If the sensed magnetic flux density of U2 is above the U2 OUT HIGH horizontal line ($B_{RP,MAX}$) in the results and it is powered, the output of U2 is assured to be high.



\square 2-16. Simulated Magnetic Flux Density Present at U1 and U2

In the results, notice that the output of U1 is not ensured to be low until the trigger is pressed at least 0.3 mm. The output on U2; however, is always asserted low as long as it is powered. If the output of U1 is not asserted low, U2 is not powered.

2.3.1.1.4.2 Placement of U3 and U4 Hall Switches

The following procedure was used to find the placement of U3 and U4:

1. An initial z-component displacement of 0 mm was selected for the z-component distance from the sensing element of switch U1 to the sensing element of switch U3. The same displacement was selected for the distance from the sensing element of switch U1 to the sensing element of switch U4.
2. An initial x-component displacement was selected for the distance from the dot on the magnet to U3. Since U3 and U4 cannot be moved in the x direction due to being surface mount parts with fixed heights, there are only two options where U3 and U4 can be placed: on the top layer or bottom layer of the PCB. Due to the placement of the PCB within the 3D printed trigger module, the shortest distance from U1 and U2 to an external magnet is when the magnet is applied underneath the trigger module as shown in \square 2-11 and \square 2-12. Consequently, U1 and U2 in this design are more affected by external magnets applied underneath the PCB and trigger module. To deal with the susceptibility of U1 and U2 to magnets applied underneath the trigger module, tamper Hall switches U3 and U4 were placed at the bottom layer of the PCB to more closely detect external magnets applied underneath the trigger module. Outside of changing the PCB layer U3 and

- U4 are placed on, the x-component displacement can also be changed by moving the magnet in the x direction. If the magnet is moved in the x direction, note that the impact of this change on the DRV5056 output must be verified if the height of the DRV5056 through-hole package cannot be adjusted accordingly.
- An initial y-component displacement was selected for the y-component distance from the sensing element of switch U1 to the sensing element of switch U3. This displacement should be far away from the trigger magnet so that it does not detect the trigger movement as an external magnetic field, but it should also be close enough to the wake-up sensor to detect nearby external magnetic fields affecting U1. [Figure 2-17](#) shows a picture of the back of the trigger module, where the back surface is removed so that the bottom of the PCB is visible. The rectangle with the “+” in it is a projection of switch 1 from its actual position on the top of the PCB to the bottom layer of the PCB that is shown in [Figure 2-17](#). The footprint of U1 is projected onto the figure to show the y and z displacements of U1 to U2 and U3.

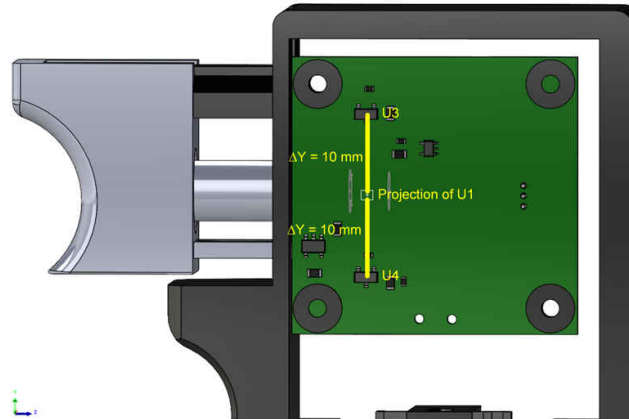


図 2-17. Placement of U3 and U4 Sensors

- After the y component of U3 was selected, a simulation was done to verify that the sensed magnetic flux density of the sensor was less than B_{OP} during the entire trigger displacement range. Additionally, the sensed magnetic flux density should be less than B_{RP} when the trigger is at rest so that the tamper outputs of the Hall sensor are automatically cleared when the trigger goes back to its rest position. If these conditions are not met, take the following actions:
 - Restart from step 3 with a different y-component displacement.
 - Restart from step 2 with a different x-component displacement. Note that the impact of this change on the DRV5056 output must be verified if the height of the DRV5056 through-hole package cannot be adjusted accordingly.
 - Modify the dimensions or material of the magnet and restart from step 2. Note that the impact of this change on the DRV5056 output must be verified.
- Repeat steps 3 and 4 but for U4 instead of U3.

Based on implementing the previous procedures, the following distances were obtained and used for this design:

- U3 distance components
 - X-component displacements
 - X-component from bottom of package to white dot of magnet = 9.40 mm
 - X-component from bottom of package to bottom of magnet = 9.40 – magnet radius = 7.02 mm
 - X-component (sensor z-offset in tool) from sensing element to bottom of magnet to sensing element = $7.02 + 0.650 = 7.67$ mm
 - Y-component displacement = +10 mm.
 - Z-component displacement (same as U1)
 - Trigger not pressed
 - Z-component from sensing element to white dot of magnet = 2.18 mm
 - Z-component from sensing element to magnet center = $2.18 - 0.5 \times \text{magnet thickness} = 2.18 - 0.5(4.76) = -0.2$ mm
 - Maximum trigger displacement = 10 mm
 - Z-component from sensing element to white dot of = 12.18 mm

- Z-component from sensing element to magnet = $12.18 - 0.5 \times \text{magnet thickness} = 12.18 - 0.5(4.76) = 9.8 \text{ mm}$
- U4 distance components
 - X-component displacements
 - X-component from bottom of package to white dot of magnet = 9.40 mm
 - X-component from bottom of package to bottom of magnet = $9.40 - \text{magnet radius} = 7.02 \text{ mm}$
 - X-component (sensor z-offset in tool) from sensing element to bottom of magnet to sensing element = $7.02 + 0.650 = 7.67 \text{ mm}$
 - Y-component displacement = -10 mm .
 - Z-component displacement (same as U1)
 - Trigger not pressed
 - Z-component from sensing element to white dot of magnet = 2.18 mm
 - Z-component from sensing element to magnet center = $2.18 - 0.5 \times \text{magnet thickness} = 2.18 - 0.5(4.76) = -0.2 \text{ mm}$
 - Maximum trigger displacement = 10 mm
 - Z-component from sensing element to white dot of = 12.18 mm
 - Z-component from sensing element to magnet = $12.18 - 0.5 \times \text{magnet thickness} = 12.18 - 0.5(4.76) = 9.8 \text{ mm}$

2.3.1.1.4.2.1 U3 and U4 Magnetic Flux Density Estimation Results

The magnetic flux density detected at switches U3 and U4 were simulated to determine appropriate placement of the Hall-effect sensors. For simulation, the distance measurements are done with respect to the sensing element to the magnet since the tool does not automatically consider the location of the sensing element within the device.

Figure 2-12 shows the corresponding magnetic flux density graphs for U3 and U4 across the travel distance of the trigger magnet.

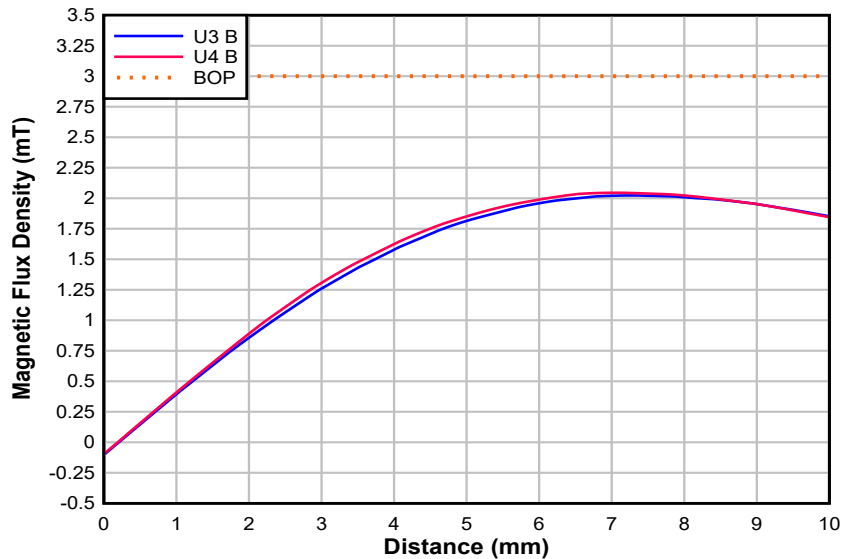


Figure 2-18. Simulated Magnetic Flux Density Detected at U3 and U4

2.3.1.1.5 Using Logic Gates to Combine Outputs from Hall-Effect Switches

If any of the tamper Hall sensors are enabled, logic gates are needed to combine the output of the multiple Hall-switches to produce one signal that provides information on whether the system should be in sleep mode. [Figure 2-19](#) shows the schematic snippet of the logic gates.

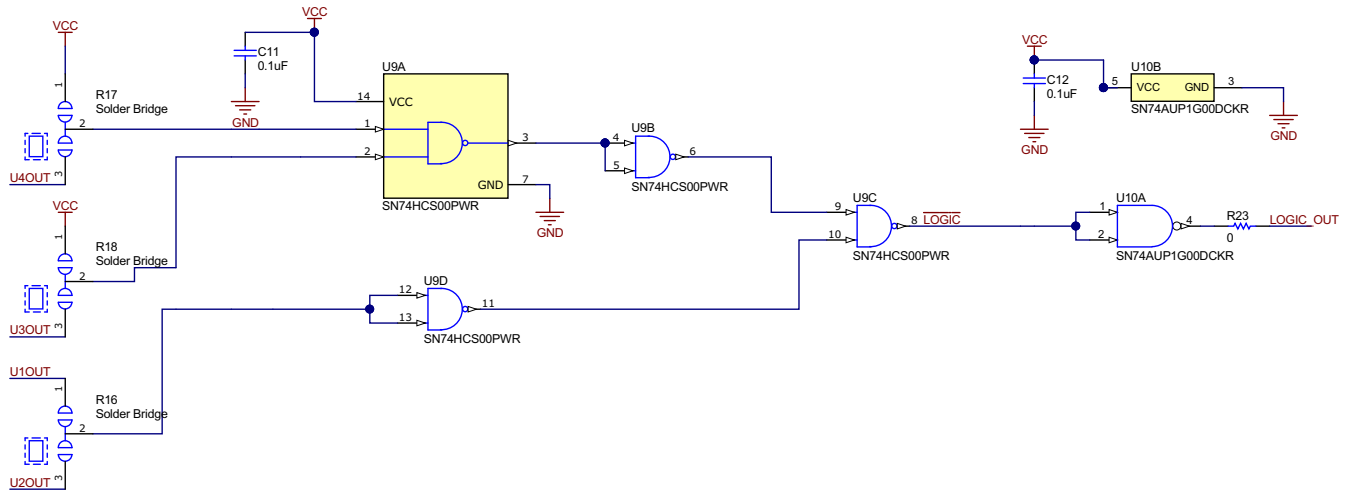


Figure 2-19. Logic Circuit Schematic

If all the Hall-switches are enabled, there are three signals that are needed to properly provide information on whether the system should be in sleep mode:

- **Switch U2's output:** The system should be placed in sleep mode if the outputs of both U1 and U2 are not asserted low. Since the GND of U2 is connected to the output of U1, the output of switch U2 is only asserted low when the output of switch U1 is asserted low.
- **Switch U3's output:** If the output of U3 is asserted low, a strong magnetic field (the field can be positive or negative) is detected, so the system should be placed in sleep mode.
- **Switch U4's output:** Similar to U3, if the output of U4 is asserted low, a strong magnetic field (the field can be positive or negative) is detected. This means the system should be placed in sleep mode.

The system should only be in active mode if the output of switch U2 is low, the output of U3 is high, and the output of U4 is high. In [Figure 2-19](#), this is implemented by using the SN74HCS00 and SN74AUP1G00 to implement the following logic function: $\overline{U2_{OUT}}U3_{OUT}U4_{OUT}$, which is output at the LOGIC_OUT signal shown in [Figure 2-19](#). The complement of this signal is also available at the LOGIC signal shown in [Figure 2-19](#). The SN74AUP1G00 is necessary since the active-high TPS22917 load switch is used. If the active-high TPS22917 load switch is replaced with the active-low TPS22916, the SN74AUP1G00 logic gate is not needed since the LOGIC signal can be connected directly to the TPS22916. [Table 2-3](#) shows the system state truth table.

Table 2-3. System State Truth Table

U2 OUTPUT ASSERTION	U3 OUTPUT ASSERTION	U4 OUTPUT	LOGIC_OUT STATE	LOGIC STATE	SYSTEM STATE	CONDITIONS
Low	Low	Low	Low	High	Sleep	External magnetic field detected by both tamper switches. The trigger is also pressed or both the stray field and wake-up sensor are fooled by an external magnet in a configuration similar to Figure 2-12 .
Low	Low	High	Low	High	Sleep	External magnetic field detected by tamper switch U3. Either the trigger is also pressed or both the stray field and wake-up sensor are fooled by an external magnet in a configuration similar to Figure 2-12 .

表 2-3. System State Truth Table (continued)

U2 OUTPUT ASSERTION	U3 OUTPUT ASSERTION	U4 OUTPUT	LOGIC_OUT STATE	LOGIC STATE	SYSTEM STATE	CONDITIONS
Low	High	Low	Low	High	Sleep	External magnetic field detected by tamper switch U4. Either the trigger is also pressed or both the stray field and wake-up sensor are fooled by an external magnet in a configuration similar to Figure 2-12 .
Low	High	High	High	Low	Active	Trigger is pressed without detecting external magnetic fields
High	Low	Low	Low	High	Sleep	External magnetic field detected by both tamper Hall switches. The trigger might not be pressed. If the trigger is pressed, both the wake-up and tamper sensors either detect a strong positive field or a strong negative field from an external source.
High	Low	High	Low	High	Sleep	External magnetic field detected by tamper switch U4. The trigger might not be pressed. If the trigger is pressed, both the wake-up and tamper sensors either detect a strong positive field or a strong negative field from an external source.
High	High	Low	Low	High	Sleep	External magnetic field detected by tamper switch U3. The trigger might not be pressed. If the trigger is pressed, both the wake-up and tamper sensors either detect a strong positive field or a strong negative field from an external source.
High	High	High	Low	High	Sleep	External magnetic field not detected by tamper switches U3 and U4. The trigger might not be pressed. If the trigger is pressed, both the wake-up and tamper sensors either detect a strong positive field or a strong negative field from an external source.

If using all the sensors is not desired, the logic gate can be configured to bypass the outputs from the Hall switches by configuring the R16, R17, and R18 3-pad footprints appropriately. By default, a 0-Ω resistor is placed at pads 2 and 3 of R16, R17, and R18, which takes the outputs from all the Hall switches and feeds it to the inputs of the logic gate. If U3 is disabled, move the 0-Ω resistor from pads 2 and 3 of R18 to pads 1 and 2, which causes the logic circuit to ignore the state of the U3 output. Similarly, if U4 is disabled, move the 0-Ω resistor from pads 2 and 3 of R17 to pads 1 and 2 so that the U3 output can be ignored by the logic circuit. If the stray field sensor is not needed, move the 0-Ω resistor from pads 2 and 3 of R16 to pads 1 and 2, which connects the output of U1 to logic circuit instead of the U2 stray-field sensor.

2.3.1.2 Linear Hall-Effect Sensor Output

Figure 2-20 shows a snippet of the DRV5056 circuit in this design. The following subsections provide details on the portions of this schematic snippet.

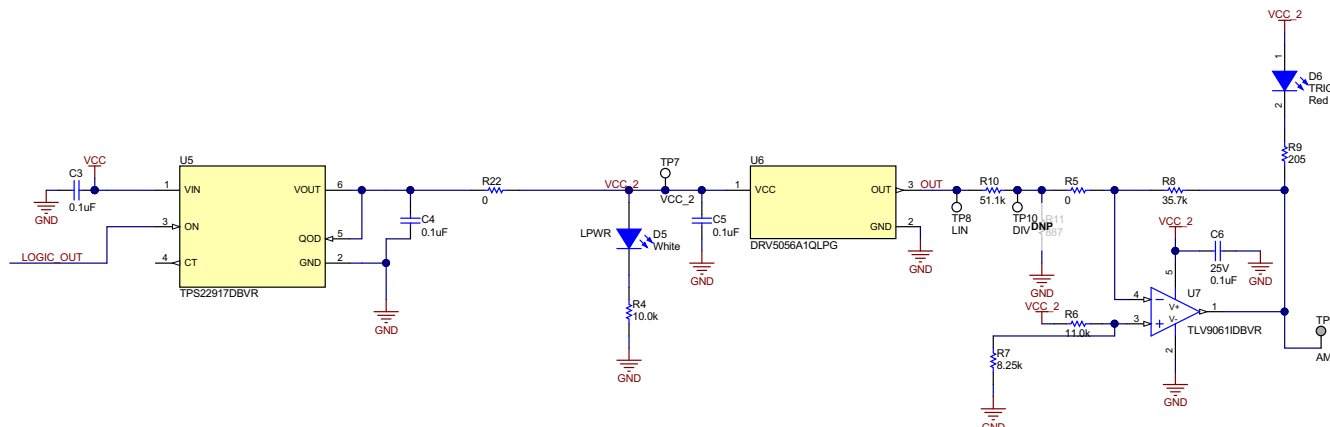


Figure 2-20. DRV5056 Schematic Snippet

2.3.1.2.1 DRV5056 Power

The DRV5056 can consume up to 10 mA, which would drain the battery if the DRV5056 was constantly powered. To reduce current consumption, the DRV5056 is powered through the TPS22917 load switch. The TPS22917 takes one of the system wake-up signals as an input. If the wake-up signal indicates that the system should be in active mode, the TPS22917 connects the VCC rail on the board to the VCC pin of the DRV5056. If the wake-up signal indicates that the system should be in sleep mode, the TPS22917 disconnects the VCC rail from the DRV5056 device, thereby preventing the DRV5056 from draining the battery when the trigger is not pressed. The LPWR D5 LED on the board indicates whether the DRV5056 is powered by turning ON when the DRV5056 is powered (active mode) and turning OFF when the DRV5056 is not powered (sleep mode).

Since the TPS22917 expects the wake-up signal to be active high but an active low signal is produced by the SN74HCS00, a SN74AUP1G00 NAND gate is used to convert the active low wake-up signal to an active high wake-up signal. Although the TPS22917 is used in this design, the board can be redesigned to replace both the active-high TPS22917 and SN74AUP1G00 with only one active-low TPS22916.

If desired, the board can also be modified to not be powered through the TPS22917 by removing R22. If R22 is removed, the DRV5056 can be powered from an external rail applied at the VCC_2 test point.

2.3.1.2.2 DRV5056 Output Voltage

The DRV5056 in this design senses the magnetic flux density produced by the trigger magnet and translates this sensed magnetic flux density into voltage using :

$$V_{\text{DRV,OUT}} = B \times S + V_Q \quad (1)$$

where

- B is the sensed magnetic flux density
- S is the sensitivity of the selected DRV5056 variant (the DRV5056A1 in this design has a typical sensitivity of 120 mV/mT at 3.3 V)
- V_Q is the quiescent voltage (0.6 V typical).

Note that the maximum recommended current that can be drawn from the DRV5056 voltage output pin is ± 1 mA, so any circuit connected to the DRV5056 output must be designed to ensure that it does not draw more than ± 1 mA from the DRV5056 OUT pin.

In this design, the D6 TRIG LED increases its brightness as the trigger is pressed. The brightness is adjusted by using a TLV9061 op-amp circuit. Resistors R6, R7, R8, and R10 were selected to translate the DRV5056 output voltage into a voltage that could drive the cathode of the LED so that the trigger magnet movement changes the intensity of this LED. The anode of D6 is connected to VCC_2, which is the switched voltage rail from the output

of the TPS22917. The voltage applied to the cathode of D6 is approximately equal to $(0.728 \times V_{CC_2}) - (V_{DRV_OUT} \times 0.699)$. As a result, the voltage across the diode will be approximately $(0.272 \times V_{CC_2}) + (V_{DRV_OUT} \times 0.699)$. The LED turns ON when the voltage across it is greater than 1.7 V. As the trigger is pressed, the voltage drop across the LED increases, thereby increasing the brightness of the LED. In addition to selecting the resistors to obtain the desired cathode voltage, these resistor values were selected so that they do not draw more than ± 1 mA from the DRV5056 output. By performing circuit simulation on this circuit, it was verified that this circuit takes less than ± 50 μ A of current from the DRV5056 OUT pin.

The TLV9061 circuit is used to drive the D6 LED for demonstration purposes when in standalone mode. It is possible to connect the DRV5056 output to an external system by removing resistor R5 so that the DRV5056 output is isolated from the TLV9061 circuit. If it is desired to divide the output from the DRV5056, resistors R10 (currently 51.1 k Ω) and R11 (currently DNP) can be replaced with values that divide the DRV5056 as needed. The output voltage from this resistor divider is brought out to the “DIV” test point on the board.

2.3.1.2.3 DRV5056 Placement

Similar to the DRV5032, the magnetic flux density detected by the DRV5056 is dependent on the magnet dimensions, magnet material, and the distance from the magnet to the sensing element within the Hall sensor. The DRV5056 device in this design uses the TO-92 through-hole package. [Figure 2-21](#) shows the location of the sensing element for this package of the DRV5056. The sensing element is located about 1.03 mm from the back side of the package. If the TO-92 width is 1.62 mm, the distance from the front of the package to the sensing element is 0.61 mm.

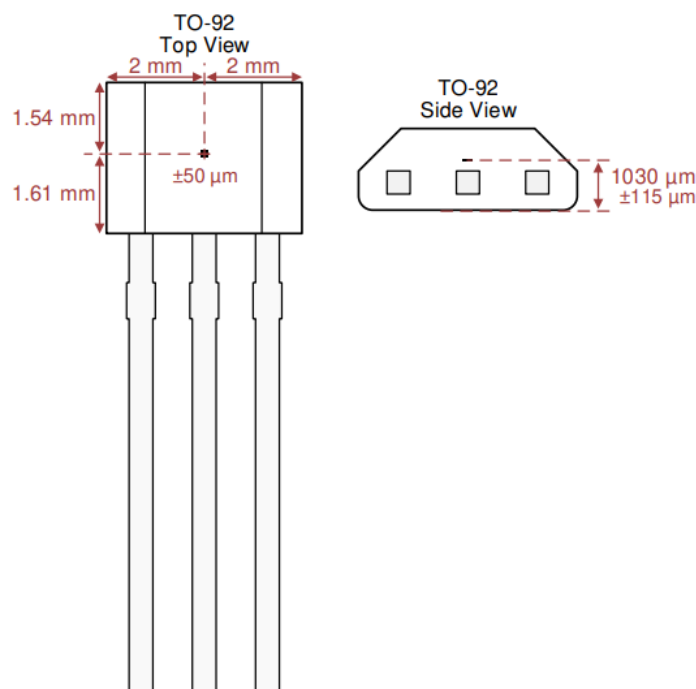


Figure 2-21. Location of Sensing Element Within TO-92 Package of DRV5056

The DRV5056 is a unipolar device that only responds to a positive field. The device detects a positive field when a south magnetic pole is near the front (marked-side) of the package, as shown in [Figure 2-22](#). The device can also detect a positive field when the north pole of a magnet is applied behind the back of the package.

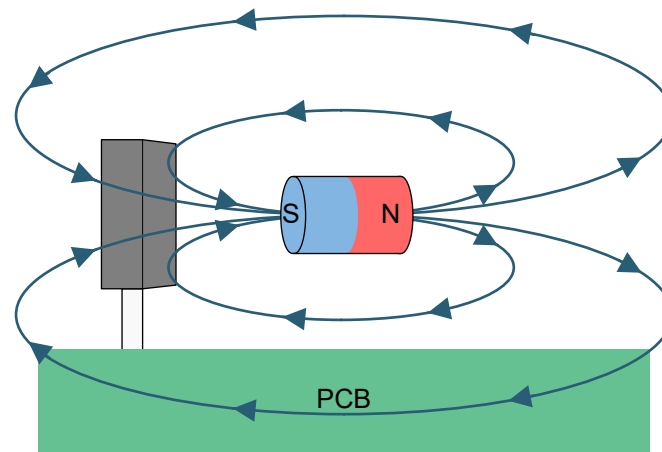


図 2-22. DRV5056 Flux Density Polarity

In this design, the north pole of the magnet is applied behind the back of the package. This made for a slightly more compact design due to the Hall element placement within the package being further from the back of the package than the front of the package. If desired, the polarity and direction of approach could be changed to a south pole from the front. If this is done, then switches U1 and U2 need to swap polarities.

Based on the magnet specifications and the distance from the magnet to the sensing elements, a calculation of the magnetic flux density was done to find a proper placement of the DRV5056 by using the [DRV5056 Distance Measurement Tool](#). This tool is able to calculate magnetic flux density for the [head-on configuration](#) used in this design, assuming that there are no x or y displacements from the center of the magnet to the sensing element. For more information, see the [Head-on Linear Displacement Sensing Using Hall-Effect Sensors](#) application brief. Since the displacement input is based on the distance from the magnet to the sensing element instead of the magnet to the top of the package, it can calculate the magnetic flux density detected when the magnet is behind the Hall sensor package as well as when the magnet is in front of the Hall sensor package.

The following procedure was used to find the placement of the DRV5056:

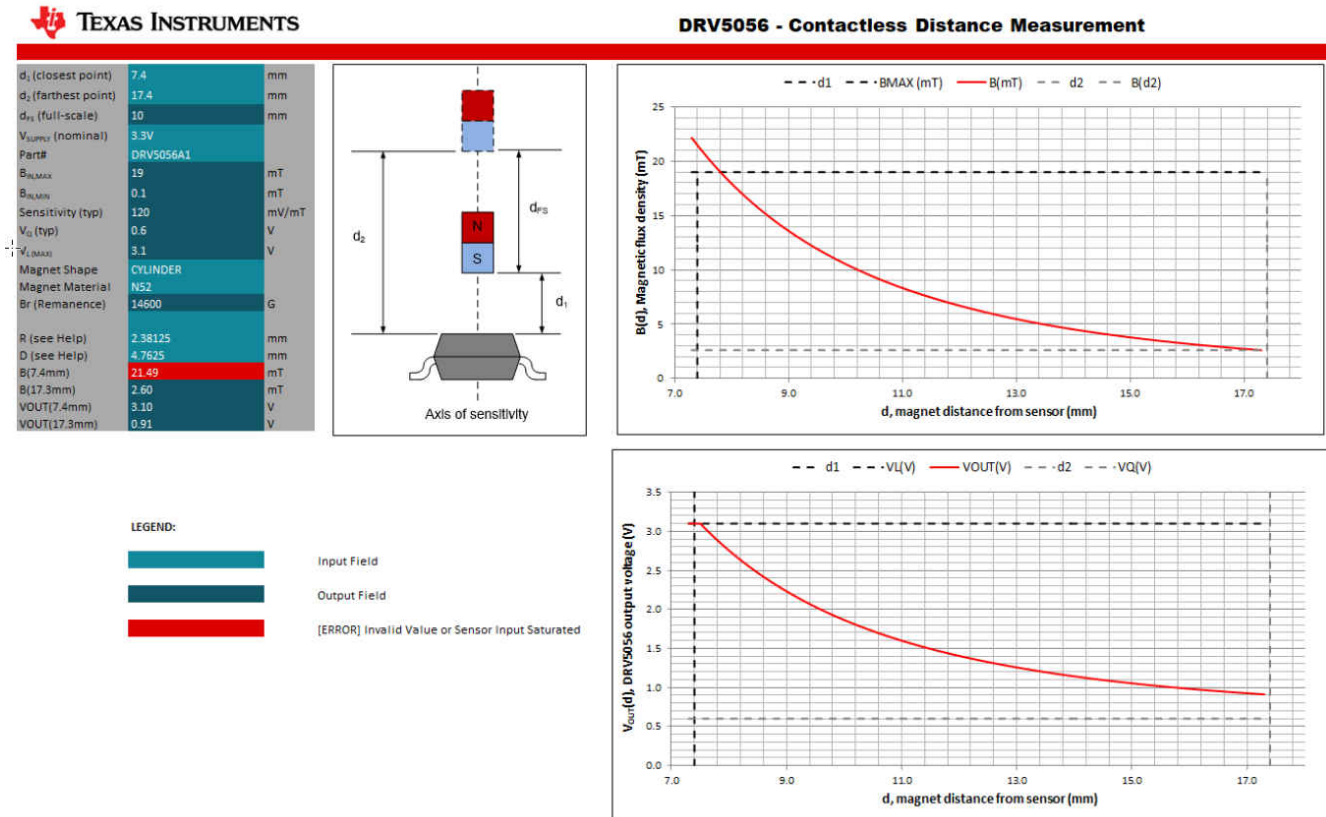
1. 0 mm is selected for the x-component and y-component displacements from the dot on the magnet in [Figure 2-14](#) to the sensing element.
2. The z-component displacement from the dot on the magnet in [Figure 2-14](#) to the sensing element was selected.
3. The DRV5056 distance measurement tool and simulations were used to estimate the magnetic flux density detected at the DRV5056 across the entire 10-mm trigger displacement distance. The DRV5056 displacement tool can be used in this case due to the x and y displacements being 0 mm. For both the distance measurement tool and the simulations, the distances from the magnet to the sensing element must be used instead of the distance from the magnet to either the front or back of the package.
4. Based on the maximum magnetic flux density estimated, the DRV5056 variant was selected so that the maximum magnetic flux density is around the maximum magnetic flux density that can be sensed by that device variant. If the estimated maximum magnetic flux density is not near the full range of any of the DRV5056 device variants, take the following steps:
 - a. Restart from step 2 with a different z-component displacement. To increase the maximum magnetic flux density by the sensor, use a smaller z displacement. To decrease the maximum magnetic flux density by the sensor, use a larger z displacement.
 - b. Modify the dimensions or material of the magnet and restart from step 2. Note that the impact of this change on the DRV5032 switch U1, U2, U3, and U4 must be verified.

Based on implementing the previous procedures, the following distances were obtained and used for this design:

- X-component displacement= 0 mm
- Y-component displacement = 0 mm
- Z-component displacement
 - Trigger not pressed
 - Z-component from white dot of magnet to back of DRV5056 package = 6.4 mm

- Z-component from white dot of magnet to sensing element (d_1 in tool) = 7.4 mm
- Maximum trigger displacement = 10 mm
- Z-component from white dot of magnet to back of DRV5056 package = 16.4 mm
- Z-component from white dot of magnet to sensing element to sensing element (d_2 in tool) = 17.4 mm

☒ 2-23 shows the settings used to estimate the magnetic flux density for the DRV5056. Once the settings have been entered into the tool, the tool calculates a table of the magnetic flux density. ☒ 2-24 is the corresponding magnetic flux density graph, which includes the magnetic flux density waveform obtained from simulation and the magnetic flux density calculated by the DRV5056 distance measurement tool. Similarly, ☒ 2-25 shows the simulated and calculated output voltage of the DRV5056.



☒ 2-23. Distance Measurement Tool Settings for DRV5056

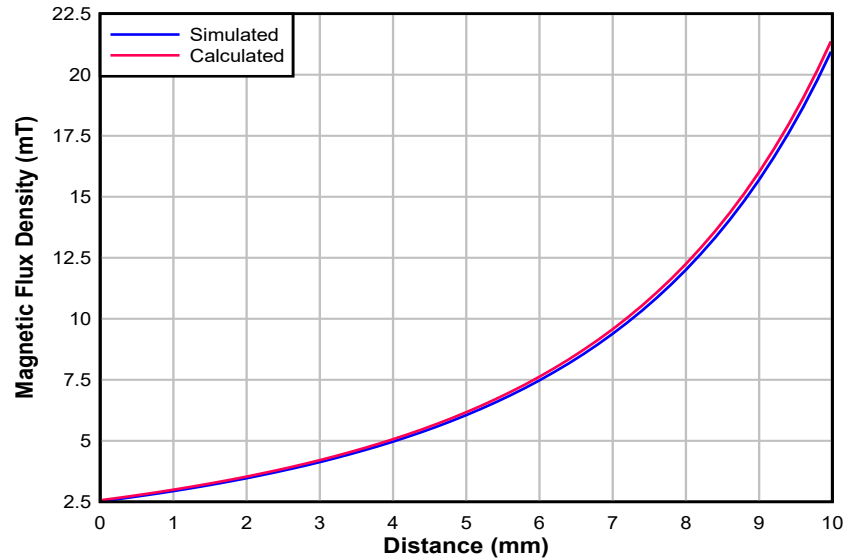


図 2-24. Simulated and Calculated Magnetic Flux Density at DRV5056

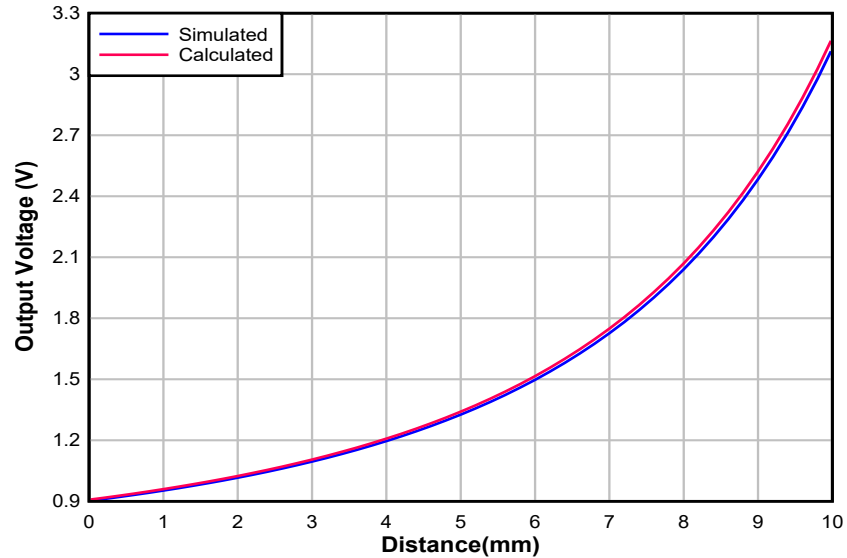


図 2-25. Simulated and Calculated DRV5056 Output Voltage

2.3.1.3 Power Supply

図 2-26 shows the power supply snippet of the schematic. The design can either be powered from an external 5-V to 30-V power supply or two AAA batteries that are inserted into the battery holder that comes with this design. The selection between these two power supply options is done by the placement of a 0-Ω resistor on two of the three pads of the R14 footprint. By default, the 0-Ω resistor is placed on pads 2 and 3 of the R14 3-pad footprint, thereby powering the design using the battery option. To power the board from the LDO, place a 0-Ω resistor on pads 1 and 2 of the R14 3-pad footprint.

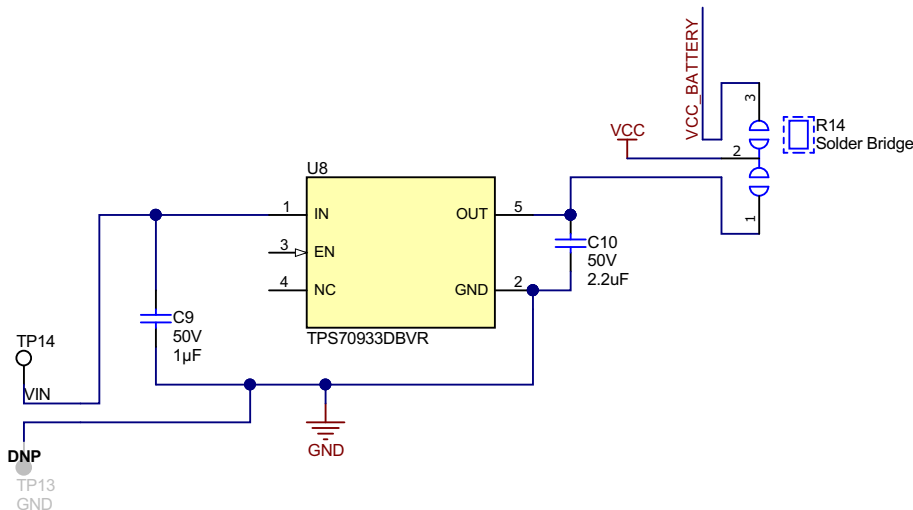


図 2-26. Power Supply Circuit

If R14 is configured to be powered from an external power supply, the positive terminal of the power supply must be connected to the VIN test point of the board and the negative terminal of the power supply must be connected to one of the GND test points on the board. The input voltage on VIN must be between 5 V to 30 V, which covers the voltage range of multiple power drill batteries. The TPS70933 LDO takes the 5-V to 30-V input and then regulates this voltage down to 3.3 V.

If the design is powered from two AAA batteries, note that the VCC rail of the board will depend on the output voltage of the AAA batteries, which will be less than 3.3 V. Since the DRV5056 has a ratiometric analog architecture that scales the sensitivity linearity with the power-supply voltage, the DRV5056 sensitivity will be scaled based on the voltage from the batteries. As an example, if the voltage from the batteries is 3.1 V instead of 3.3 V, the sensitivity at 3.1 V would be about 94% of the sensitivity at 3.3 V. For the A1 device variant used in this design, this means that the sensitivity would be about 112.7 mV/mT typical instead of the 120 mV/mT sensitivity seen at 3.3 V.

2.3.1.4 Transistor Circuit for Creating High-Voltage Enable Signal

The design has an optional transistor circuit (shown in 図 2-27) that can be used for creating a high-voltage signal that provides information on whether the system is in sleep or wake mode. This circuit takes the active-low output signal from the SN74HCS00 logic gate and produces an active-high, high-voltage version of this signal.

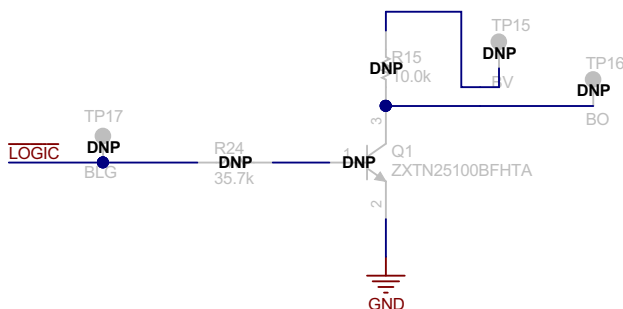


図 2-27. Transistor Circuit

The circuit in 図 2-27 was added in case it is desired to emulate connecting or disconnecting the battery from a signal based on the sleep state. This signal can be used to put an external system to sleep if that external system goes to sleep mode based on the state of a high-voltage pin.

To use this circuit, populate R24, Q1, and R15. Next, apply the high-voltage input on the BV test point. This high-voltage input is the voltage that the output enable signal should be referenced with respect to. As an example, connect this high-voltage input to the power drill battery to create an enable signal that is referenced with respect to the battery in the drill. The output signal is produced on the BO test point. If the system is in sleep mode, the

voltage at BO is equal to 0 V. If the system is in active mode, the voltage at BO is set to the voltage applied at BV.

The circuit in [Figure 2-27](#) is mainly for demonstration purposes. To reduce system current consumption, note that circuit is not populated by default. Also note that the produced enable signal is not meant to power a drill or any other system. The signal is primarily intended to trigger other components that actually connect or disconnect power to the system, such as an external high current eFuse, load switch, or hot-swap controller.

2.3.2 Alternative Implementations

2.3.2.1 Replacing 20-Hz Tamper Switches With 5-Hz Tamper Switches

In this reference design, the SOT-23 version of the DRV5032FA device variant is used for switches U3 and U4; however, if the response time of the tamper Hall sensors is not important, these switches can be replaced with the SOT-23 version of the DRV5032FB device variant for a reduced current consumption. The SOT-23 packages of these two device variants only vary in terms of sampling rate; the other device parameters are the same.

[Figure 2-28](#) shows the typical magnetic sampling period and average current consumption of the FA and FB devices from the data sheet. The response time of the DRV5032FB is 200 ms compared to the 50 ms response time of the DRV5032FA. In systems that can use a tamper sensor that has a 200 ms response time, using the DRV5032FB can reduce the typical average current consumption of each Hall sensor from 1.6 μA to 0.7 μA . As a result, using the DRV5032FB for both U3 and U4 can reduce the sleep current consumption of the design by up to 1.8 μA .

DU, FA, FC, FD, AJ, ZE VERSIONS						
f_s	Frequency of magnetic sampling		13.3	20	37	Hz
t_s	Period of magnetic sampling		27	50	75	ms
$I_{CC(AVG)}$	Average current consumption	$V_{CC} = 1.8\text{ V}$		1.3		μA
		$V_{CC} = 3\text{ V}$		1.6	3.5	
		$V_{CC} = 5\text{ V}$		2.3		
FB VERSION						
f_s	Frequency of magnetic sampling		3.5	5	8.5	Hz
t_s	Period of magnetic sampling		117	200	286	ms
$I_{CC(AVG)}$	Average current consumption	$V_{CC} = 1.8\text{ V}$		0.54		μA
		$V_{CC} = 3\text{ V}$		0.69	1.8	
		$V_{CC} = 5\text{ V}$		1.06		

Figure 2-28. Current Consumption of Different DRV5032 Variants

2.3.2.2 Using Shielding to Replace Tamper Switches and Stray Field Switch

Switches U2, U3, and U4 are included for added protection against external magnetic fields. An alternative method that can be used to make designs immune against external magnetic fields is adding magnetic shielding to the design. Note that magnetic shielding is a way of creating an alternative path for magnetic flux to flow and is not getting rid of the flux. The shield is made of a highly permeable material, which provides a preferential path for the flux to pass through. One disadvantage of shielding, however, is that it not only affects external magnetic fields; it can also affect the internal magnetic fields generated by the trigger magnet, thereby affecting the measurement of the magnetic flux density of the linear Hall-effect sensor. Consequently, for shielding to be used, it must be verified that the shielding does not significantly affect the measurement of the magnetic field of the linear Hall-effect sensor from the trigger magnet.

If magnetic shielding is implemented successfully in a design, it could replace the two tamper Hall switches, stray field switches, and the logic gates in this design (see [Figure 2-29](#)), thereby reducing current consumption. However, shielding may also increase the weight of the system.

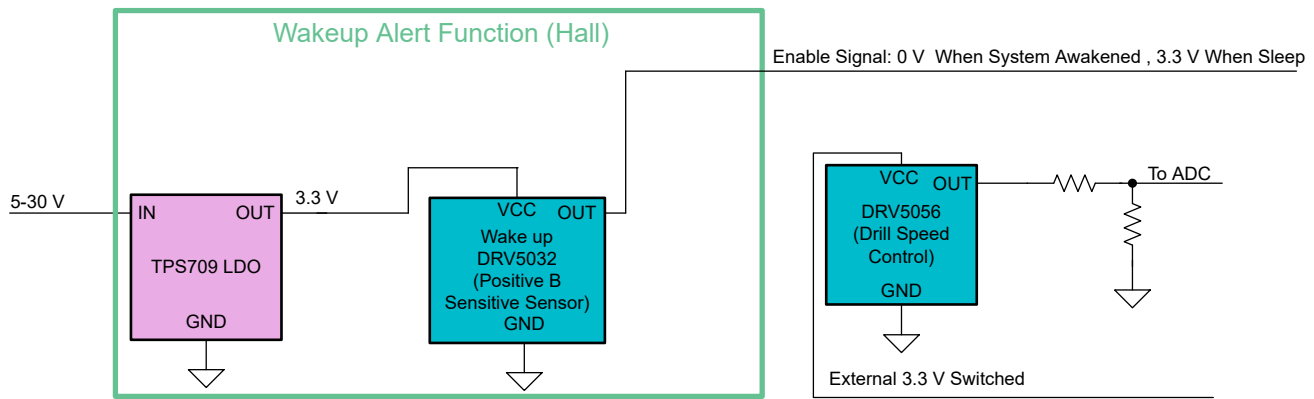


図 2-29. Block Diagram of Solution With Shielding

2.3.2.3 Replacing Hall-Based Wake-Up Alert Function With a Mechanical Switch

In this design, a Hall-based implementation is used for both waking up the system and translating the trigger displacement into an output voltage. However, a hybrid approach is also possible, where a mechanical switch wakes up the system when the trigger is pressed and a linear Hall-effect sensor translates the trigger displacement into an output voltage. This alternative architecture essentially replaces the entire Hall-based wake-up alert function (the green box within the block diagram in 図 2-1) with a mechanical switch. By replacing the wake-up alert function with a mechanical switch, the following components are not needed (see 図 2-30):

- Wake-up DRV5032 sensor (U1)
- Stray Field Sensor (U2)
- Tampering Hall sensor for preventing accidental wake ups (U3 and U4)
- SN74HCS00 and SN74AUP1G00 logic gates for combining the outputs from the different Hall switches
- TPS709 LDO to power the always-on Hall-sensors. The mechanical switch can be referenced with respect to the battery voltage and does not need regulation.
- TPS22917 (this was mainly present for demo purposes in standalone mode). If the external system already has an internally-generated voltage rail that is disabled or enabled based on whether the system is in sleep mode, this rail can power the DRV5056.
- NPN transistor switch circuit. If the mechanical switch is referenced with respect to the power tool battery, it is not necessary to create another high-voltage enable signal.

By removing the previously-listed components, this hybrid approach can obtain a reduced system current consumption than this design. However, the mechanical switch would have more issues with wear and tear compared to the approach used in this design, which could reduce the lifetime of systems build with this hybrid mechanical switch + linear Hall-effect sensor approach compared to the Hall-effect switch + linear Hall-effect sensor architecture used in this design.

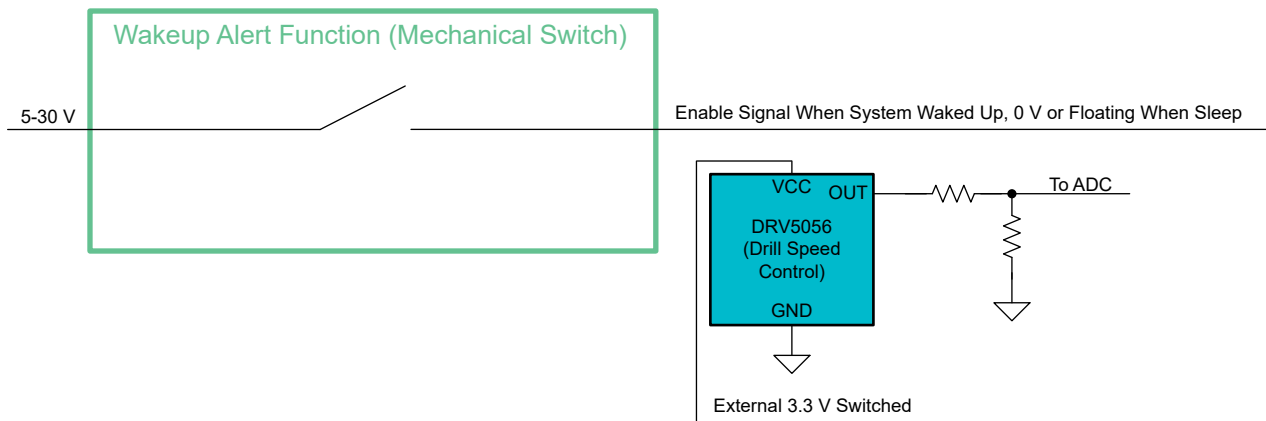


図 2-30. Block Diagram of Mechanical Switch + Linear Hall Sensor Solution

3 Hardware, Software, Testing Requirements, and Test Results

3.1 Hardware Requirements

3.1.1 Installation and Demonstration Instructions

This hardware comes with an empty battery holder that is placed inside the 3D printed trigger module. [Figure 3-1](#) shows the 3D model of the trigger module (note that the spring and the battery holder wires are not shown in the image).

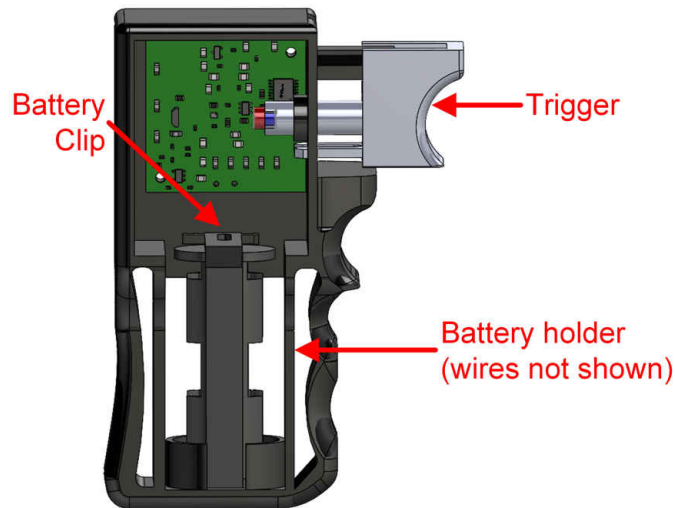


Figure 3-1. Front View With Battery Holder Inside Trigger Module

To use this design, batteries must be placed inside the battery holder. Batteries can be installed by first pushing the battery clip upwards and simultaneously taking the battery holder outside of the trigger module. [Figure 3-2](#) shows a 3D model with the battery holder placed outside the trigger module. After the battery holder is outside the trigger module, install the two AAA batteries into the battery holder. Finally, the battery holder should be placed back into the trigger module by pressing the clip upwards while placing the battery holder back into the trigger module until the battery holder is inside the trigger module again (see [Figure 3-1](#)).

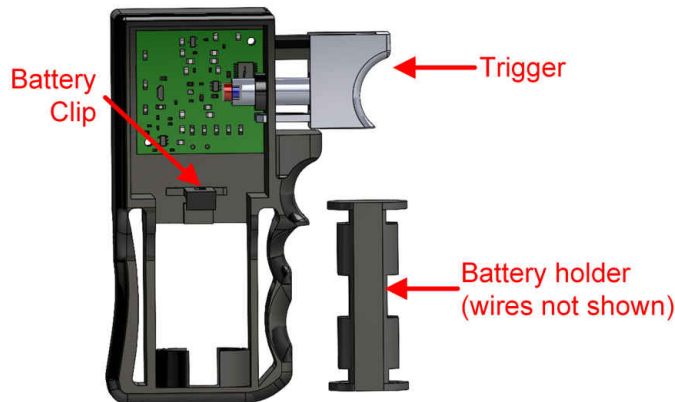


Figure 3-2. Front View With Battery Holder Outside Trigger Module

The design can be used in standalone mode by pressing the trigger in [Figure 3-1](#) to the left and observing the state of the LEDs on the board. When the trigger displacement reaches a certain distance threshold, the system is awakened from sleep mode. LEDs D1, D2, and LPWR will be ON when the system is in active mode and LEDs D3 and D4 will be OFF. In addition, the TRIG LED will change its brightness based on how far the trigger is pressed. The further the trigger is pressed, the brighter the TRIG LED will appear. Note that the trigger cannot be

pressed to reach a full displacement distance of 10 mm due to the spring preventing the trigger from being fully pressed.

If an external magnetic field is detected by switch U3, LED U3 will be on and the system will be placed in sleep mode. Similarly, if an external magnetic field is detected by switch U4, LED U4 will be turned ON and the system will also be placed in sleep mode. As an alternative to viewing the state of the LED, the outputs of the different Hall sensors can also be observed by measuring the output voltage at the corresponding test points on the board. [セクション 3.1.2](#) provides more details on the test points and LEDs available on this board.

3.1.2 Test Points and LEDs

表 3-1. LEDs

LED	PURPOSE
D1	This LED is connected to the output of U1. The LED is turned ON when the output is asserted low and turned OFF when the output is asserted high.
D2	This LED is connected to the output of U2. The LED is turned ON when the output is asserted low and turned OFF when the output is asserted high.
D3	This LED is connected to the output of U3. The LED is turned ON when the output is asserted low and turned OFF when the output is asserted high. If U3 detects an external magnetic field, this LED is turned ON.
D4	This LED is connected to the output of U4. The LED is turned ON when the output is asserted low and turned OFF when the output is asserted high. If U4 detects an external magnetic field, this LED is turned ON.
D5 (labeled LPWR on board)	This LED is connected to the VCC pin of the DRV5056 and provides info if the system is in sleep or active mode. The system is only in active mode if LEDs D1 and D2 are ON while LEDs D3 and D4 are OFF.
D6 (labeled TRIG on board)	This LED changes its brightness based on how far the trigger is pressed. The further the trigger is pressed, the brighter this LED.

表 3-2. Test Points

DESIGNATOR	BOARD LABEL	PURPOSE
TP1	VCC	Main power supply of the board. This is either connected to the TPS709 output or the positive terminal of the battery placed in the battery holder.
TP2, TP3, TP4, TP13	GND	Board GND
TP5	SW1	Output of switch U1
TP6	SW2	Output of switch U2
TP7	VCC_2	VCC pin of DRV5056. When the trigger is not pressed, this is disconnected from VCC (test point TP1) on the board. When the trigger is pressed, VCC_2 is connected to VCC through the TPS22917 load switch.
TP8	LIN	Output of DRV5056
TP9	AMP	Output of TLV9061, which drives the cathode of the TRIG (L6) LED so that it changes its brightness based on how far the trigger is pressed.
TP10	DIV	If R10 and R11 are used to divide the output voltage from the DRV5056, this is the divided down voltage. By default, the voltage divider is not enabled. To enable it, the op-amp circuit must be disabled by removing resistor R5 from the board.
TP11	SW4	Output of switch U4
TP12	SW3	Output of switch U3
TP14	VIN	LDO input. When the board is powered from an external power supply, this test point is connected to the external 5-V to 30-V power supply so it can regulate the voltage to 3.3 V.
TP15	BV	Connected to the voltage that you want enable signal option 2 to be referenced with respect to. This can be connected to the cordless power tool battery so that enable signal is referenced with respect to the high voltage. By default, the enable signal option 2 is not available due to this circuit not being populated.

表 3-2. Test Points (continued)

DESIGNATOR	BOARD LABEL	PURPOSE
TP16	BO	Enable signal option 2. By default, the enable signal option 2 is not available due to this circuit not being populated. If the system is in active mode, the voltage here is equal to BV. If the system is in sleep mode, the voltage here is at 0 V.
TP17	LOGIC	Enable signal option 1. This is taken from the SN74HCS00 output. This is available by default. If the system is in active mode, this test point is at 0 V. If the system is in sleep mode, the voltage of this test point is set to the VCC voltage.

3.1.3 Configuration Options

3.1.3.1 Disabling Hall-Effect Switches

Switches U2, U3, and U4 can be disabled to reduce current consumption when protection against external magnetic fields is not necessary.

The different switches can be disabled by performing the following:

- **Disabling U2:** Remove resistor R21. Move the 0-Ω resistor on the 3-pad R16 footprint from pads 2 and 3 to pads 1 and 2.
- **Disabling U3:** Remove resistor R20. Move the 0-Ω resistor on the 3-pad R18 footprint from pads 2 and 3 to pads 1 and 2.
- **Disabling U4:** Remove resistor R19. Move the 0-Ω resistor on the 3-pad R17 footprint from pads 2 and 3 to pads 1 and 2.

The switches can be enabled again by doing the following:

- **Enabling U2:** Place a 0-Ω resistor at R21. Move the 0-Ω resistor on the 3-pad R16 footprint from pads 1 and 2 to pads 2 and 3.
- **Enabling U3:** Place a 0-Ω resistor at R20. Move the 0-Ω resistor on the 3-pad R18 footprint from pads 1 and 2 to pads 2 and 3.
- **Enabling U4:** Place a 0-Ω resistor at R19. Move the 0-Ω resistor on the 3-pad R17 footprint from pads 1 and 2 to pads 2 and 3.

3.1.3.2 Configuring Hardware for Standalone Mode or Connection to External Systems

This design can operate in standalone mode (this is the default configuration), which does not need to be connected to an external system, or some of the signals from the design can be connected to an external signal.

In standalone mode, the trigger LED is mainly used to indicate how far the trigger is pressed. To configure the design for full standalone mode, use the following configuration:

- Ensure that a 0-Ω resistor is on pads 2 and 3 of the 3-pad R14 footprint. This configures the design to operate off the batteries placed in the battery holder.
- Ensure that a 0-Ω resistor is at R22. This allows the DRV5056 to be powered when the trigger is pressed and unpowered when the trigger is not pressed.
- Ensure that a 0-Ω resistor is at R5 so that the brightness of the TRIG LED changes based on how far the trigger is pressed.

The design also has various options to support connecting to an external system, including the following:

- **Operation from an external power supply, such as an 18-V cordless power tool battery:** To operate from an external power supply, ensure that a 0-Ω resistor is on pads 1 and 2 of the 3-pad R14 footprint. The positive terminal of the power supply is connected to the LDOIN test point and the negative terminal of the power supply is connected to any of the GND test points.
- **Powering the DRV5056 from an external power supply:** The DRV5056 can be powered from an external power supply. An example use-case is when the DRV5056 will be powered from an external voltage rail that is switched ON or OFF based on whether the external system should be in sleep mode or active mode. Another use-case is for powering the DRV5056 from the same VCC voltage rail that powers the ADC that measures the output voltage of the DRV5056. The DRV5056 uses a ratiometric architecture that can reduce error from VCC tolerance when the external analog-to-digital converter (ADC) uses the same VCC for its

reference, so connecting the ADC VCC to the DRV5056 can reduce error. To power the DRV5056 from an external power supply, remove the resistor at R22 so that the DRV5056 is not powered through the TPS22917. Next, connect the positive terminal of the external power supply to the VCC_2 test point and the negative terminal of the power supply to any of the GND test points. To power the DRV5056, the power supply must be at either 3 V to 3.6 V or 4.5 to 5.5 V. In addition, the power supply must be able to power a 10-mA load.

- **Connecting the DRV5056 output to an external system:** The DRV5056 can be connected to an external system by removing resistor R5. By doing this, note that the op-amp circuit is disabled and the TRIG LED does not change its brightness based on how far the trigger is pressed; however, the DRV5056 still changes based on how far the trigger is pressed. If desired, resistors R10 and R11 can also be populated to scale down the output voltage from the DRV5056, which allows the DRV5056 output to be scaled down to match the input voltage of ADCs with a relatively small input voltage range. The undivided DRV5056 output voltage is available on the LIN test point and the scaled down voltage is available on the DIV test point. In addition to connecting to the LIN or DIV test points to the external system, the GND of this design should also be connected to the GND of the external system.
- **Providing wake-up signal to an external system (enable signal option 2):** The design has a transistor circuit that translates the wake-up signal used internally in the design (enable signal option 1) into a wake-up signal that is used externally (enable signal option 2). One use-case for this is for interfacing to external systems that require a system wake-up signal that is shorted to the battery whenever the system should be in active mode and disconnected from the battery when the system is in sleep mode. The transistor circuit can emulate connecting and disconnecting the battery to a wake-up signal within the external system. By default, the circuit for enable signal option 2 is not populated in this design. So to use this option, R24, Q1, and R15 must be populated. After populating these components, the voltage that the signal is referenced to should be applied to the BV test point. As an example, connect this high-voltage input to the power drill battery to create an enable signal that is referenced with respect to the battery in the drill. The output signal is produced on the BO test point. BO equals 0 V when the system is in sleep mode and it equals the voltage set at BV when the system is in active mode. Note that the produced enable signal is not meant to power anything that draws a lot of current. Enable signal option 2 is primarily intended to trigger other components that actually connect or disconnect power to the system, such as an external high current eFuse, load switch, or hot-swap controller.

3.2 Test Setup

3.2.1 Output Voltage Accuracy Testing

To precisely control the positioning of the trigger magnet with respect to the DRV5056, a motion controller system was used instead of doing testing using the 3D printed module. The motion controller consisted of a moving plate and a fixed plate, where the distance between the plates can be precisely controlled. In this setup, a magnet holder was 3D printed to hold the trigger magnet. The magnet holder was placed on the moving plate and the board of the design was placed on top of the fixed plate, as shown in [Figure 3-3](#). Once the board was placed, an external 3.3-V power supply was connected to it.

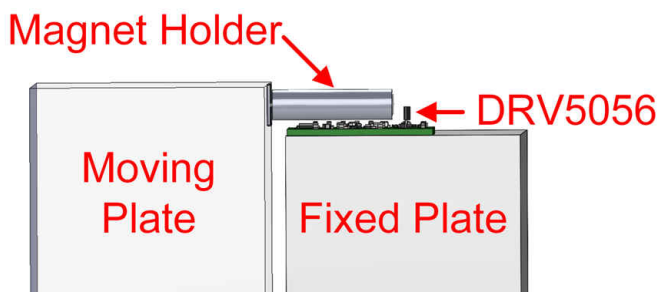


Figure 3-3. Test Setup

After the magnet and board was placed, a correction factor was determined to convert the distance between the plates into the distance between the magnet and the DRV5056 sensing element. Using the conversion factor, the plate was moved so that the magnet was 7.4 mm from the sensing element of the DRV5056 (6.4 mm from the back of the DRV5056 package). This 7.4 mm distance corresponds to a trigger displacement of 10 mm. A multimeter then measured the voltage on the "LIN" test point, which is directly connected to the DRV5056

output. For this test, note that the LED op-amp circuit was disabled as a precaution by removing resistor R5, so the op-amp circuit did not draw current from the DRV5056 output. After taking a reading at 7.4 mm, readings were taken every 0.2 mm until the final reading at 17.4 mm was taken. The 17.4 mm distance corresponds to a trigger displacement of 0 mm.

Next, the design was calibrated. During calibration, the expected magnetic flux densities and measured output voltages were used to calculate new values for the sensitivity and quiescent voltage. The measured voltages were then converted to corrected magnetic flux density values using the new sensitivity and quiescent voltage values using the following formula: $B_{\text{corrected}} = (V_{\text{measured}} - V_{Q, \text{corrected}}) / \text{Sensitivity}_{\text{corrected}}$. To calculate the corrected voltage, the corrected magnetic flux density used the ideal values of the sensitivity and quiescent voltage: $V_{\text{corrected}} = (B_{\text{corrected}} \times \text{Sensitivity}_{\text{ideal}}) + V_{Q, \text{ideal}} = (B_{\text{corrected}} \times 0.12) + 0.6$.

Testing was done with four different calibration options to show the accuracy of each option. The following calibration options were specifically tested:

- **1 line, 2-point calibration:** This calibration was performed using two data points to calculate a best-fit line equation. The slope of the best-fit line equation was selected for $\text{Sensitivity}_{\text{corrected}}$ and the y-intercept of the line was selected for $V_{Q, \text{corrected}}$. The values of $\text{Sensitivity}_{\text{corrected}}$ and V_Q were applied to all the data points from 0 to 10 mm. The selected two data points were taken at 7.8 mm and 17.2 mm. The value of 7.8 mm was selected as a calibration point because it was the first data point where the DRV5056 was powered. At 7.4 mm to 7.8 mm, the DRV5056 was turned OFF. The value of 17.2 mm was selected as the second calibration point because the data point at 17.4 mm was near the outside of the nonlinear output range of the DRV5056.
- **1 line, 3-point calibration:** This calibration option uses three points to calculate the best-fit line instead of two. In addition to the two data points used in the 1 line, 2-point calibration option, a third calibration point at 12.2 mm was used as well.
- **2 line, 2-point calibration :** This option calculates two different sets of $\text{Sensitivity}_{\text{corrected}}$ and V_Q values. The first set of values, $\text{Sensitivity}_{\text{corrected},1}$ and $V_{Q,1}$, were calculated using the data at 17.2 mm and 12.6 mm. The second set of values, $\text{Sensitivity}_{\text{corrected},2}$ and $V_{Q,2}$, were calculated using the data at 12.4 mm and 7.8 mm. Data points from 17.4 to 12.6 mm were corrected using the values of $\text{Sensitivity}_{\text{corrected},1}$ and $V_{Q,1}$ while data points from 7.4 to 12.4 mm were corrected using the values of $\text{Sensitivity}_{\text{corrected},2}$ and $V_{Q,2}$.
- **4-line, 2-point calibration :** This option calculates four different sets of $\text{Sensitivity}_{\text{corrected}}$ and V_Q values. The first set of values, $\text{Sensitivity}_{\text{corrected},1}$ and $V_{Q,1}$, were calculated using the data at 17.2 mm and 15 mm. These first set of values are used to calculate corrected data points from 15 mm to 17.4 mm. The second set of values, $\text{Sensitivity}_{\text{corrected},2}$ and $V_{Q,2}$, were calculated using the data at 14.8 mm and 12.6 mm. These values corrected 12.6 mm to 14.8 mm. The third set of values, $\text{Sensitivity}_{\text{corrected},3}$ and $V_{Q,3}$, were calculated using the data at 12.4 mm and 10.2 mm. These third set of values corrected the data points from 10.2 to 12.4 mm. The last set of values, $\text{Sensitivity}_{\text{corrected},4}$ and $V_{Q,4}$, were calculated using the data at 10 mm and 7.8 mm. These last set of correction values corrected data points that were less than 10.2 mm.

The pre-calibration % error of the measurements were then calculated by comparing the measured data with the corresponding values from simulation and the DRV5056 distance measurement tool. The post-calibration % error was calculated using the corrected voltage values and the corresponding voltage values from simulation and the DRV5056 distance measurement tool. The following post-calibration % error calculations were done:

- Simulated (1 line, 2-point): % error calculation using the voltages from simulation and the 1 line, 2-point corrected voltage
- Calculated (1 line, 2-point): % error calculation using the voltages from the DRV5056 measurement tool and the 1 line, 2-point corrected voltage. Note that the corrected voltage values here were corrected based on the DRV5056 measurement voltage values instead of the voltage values from simulation. As a result, the corrected voltage is different than the corrected voltage used in the 1 line, 2-point simulated scenario.
- Simulated (1 line, 3-point): % error calculation using the voltages from simulation and the 1 line, 3-point corrected voltage
- Simulated (2 line, 2-point): % error calculation using the voltages from simulation and the 2 line, 2-point corrected voltage
- Simulated (4 line, 2-point): % error calculation using the voltages from simulation and the 4 line, 2-point corrected voltage

3.2.2 Magnetic Tampering Testing

Magnetic tampering testing was performed by using a strong 0.5 in diameter × 1.5 in thick N52 cylinder magnet. The magnet was applied underneath the trigger module because that location is most susceptible to external magnetic fields due to that location having the shortest possible distance from the Hall sensors to any external magnets that are placed on the trigger module.

The two magnet orientations shown in [Figure 2-11](#) and [Figure 2-12](#) were tested. For the different magnet orientations of the external magnet, it was verified that the system did not turn ON by making sure that the LPWR LED did not turn ON. For more information on which Hall sensors were triggered by the different magnet orientations, the individual LEDs on switches U1, U2, U3, and U4 were also observed.

3.2.3 Current Consumption Testing

Before performing current consumption testing, the following board changes were made to ensure that the current consumption measurements did not include the components on the design that were mainly used for demonstration purposes and would not be implemented in a final system:

- BJT Q1, resistor R25, and resistor R15 were removed
- The individual LEDs on switches U1, U2, U3, and U4 were removed

After making these changes, the trigger design was powered from a DC power analyzer that would also measure the current consumption. The design was powered using one of the three options:

- Using the LDO with 5 V applied to its input
- Using the LDO with 18 V applied to its input
- Bypassing the LDO by removing it from the board and applying 3.3 V directly to VCC

The average current consumption was measured under the following conditions:

- Condition 1: All Hall sensors enabled
- Condition 2: Tamper Hall switch U3 disabled
- Condition 3: Tamper Hall switches U3 and U4 disabled
- Condition 4: Stray field switch U2, tamper Hall switch U3, and tamper Hall switch U4 disabled
- Condition 5: LDO, Stray field switch U2, tamper Hall switch U3, and tamper Hall switch U4 disabled.

3.3 Test Results

3.3.1 Output Voltage Accuracy Pre-Calibration Results

The graphs in [Figure 3-4](#) and [Figure 3-5](#) express the distance in terms of displacement from the trigger resting point. The 0 mm value in the graphs corresponds to a distance of 17.4 mm between the magnet to the DRV5056 sensing element and 10 mm corresponds to a distance of 7.4 mm. Also, note that the system does not turn ON until the trigger is pressed 0.4 mm. As a result, the DRV5056 does not translate the sensed magnetic flux density into voltage until 0.4 mm.

Without doing calibration, the worst observed error between the measured voltage and the simulated voltage is – 2.6%.

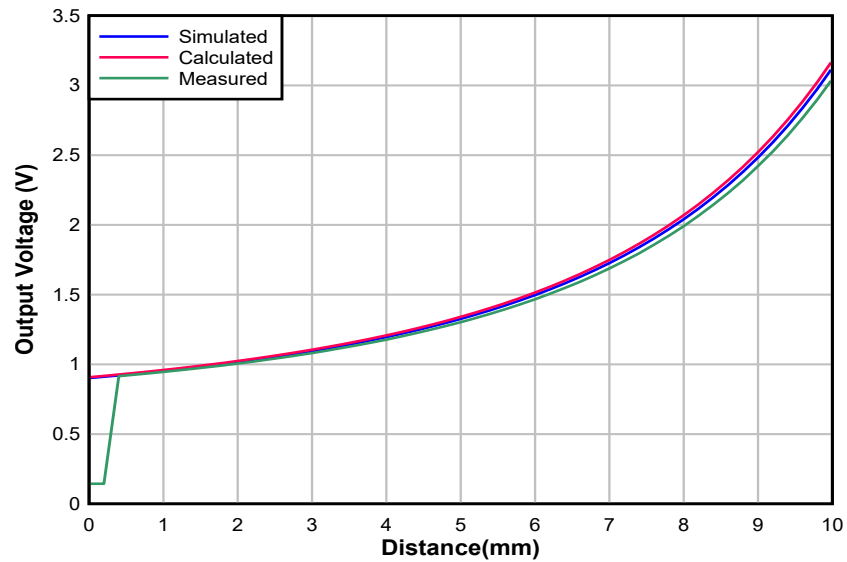


図 3-4. DRV5056 Output Voltage vs Trigger Displacement Distance (Before Calibration)

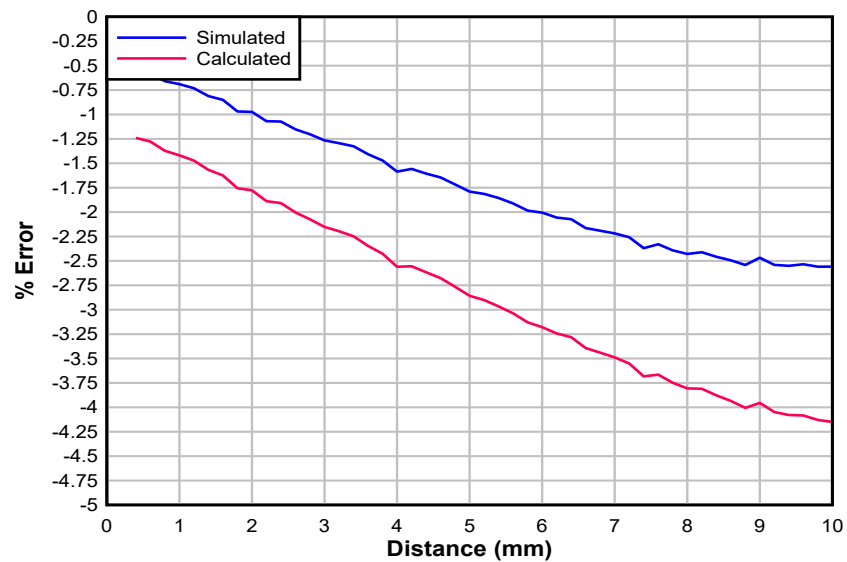


図 3-5. DRV5056 Output Voltage % Error vs Trigger Displacement Distance (Before Calibration)

3.3.2 Output Voltage Accuracy Post-Calibration Results

図 3-6 shows the DRV5056 output voltage versus trigger displacement distance after calibration.

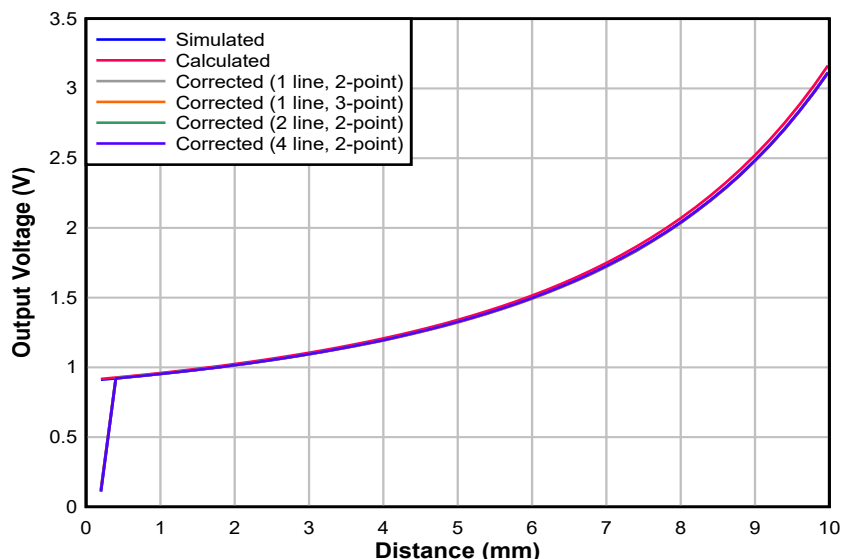


図 3-6. DRV5056 Output Voltage vs Trigger Displacement Distance (After Calibration)

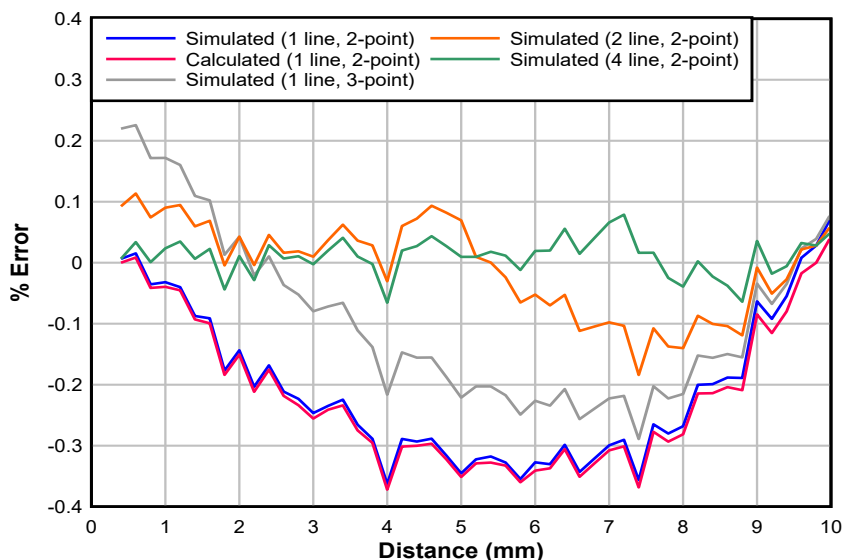


図 3-7. DRV5056 Output Voltage % Error vs Trigger Displacement Distance (After Calibration)

表 3-3 shows the worst observed error in 図 3-7. The post-calibration error is affected by noise, linearity error, and possible magnet positioning errors. To reduce the impact of linearity error, calibration was done using multiple points and lines. Additional averaging of the sample data can be done to reduce noise.

表 3-3. Post-Calibration Worst Observed Error

CONDITION	ABSOLUTE VALUE OF WORST OBSERVED ERROR
Simulated (1 line, 2-point)	0.363%
Calculated (1 line, 2-point)	0.372%
Simulated (1 line, 3-point)	0.289%
Simulated (2 line, 2-point)	0.184%
Simulated (4 line, 2-point)	0.0789%

From the results, the 1 line, 3-point calibration provides a reduced worst-observed error than the 1 line, 2-point calibration. Note that the utilized best-fit line algorithm works by minimizing the sum of the squared errors instead

of minimizing the worst observed error. As a result, using more points for the best-fit line may not always result in a reduction of the worst observed error as it did in this case.

In addition, increasing the number of lines from 1 to 2 to 4 also reduces the worst observed error.

3.3.3 Magnetic Tampering Results

When the external magnet was applied to the trigger module according to the orientation shown in [Figure 2-11](#), the system did not turn ON. The external magnet caused the output of the wake-up sensor to be asserted low due to the sensor detecting a strong positive field; however, the system remained OFF since the external magnet caused the stray field sensor to also detect a strong positive field instead of the negative field needed to turn the system ON.

The external magnet was also applied to the trigger module according to the orientation shown in [Figure 2-12](#). In this orientation, the output of both the wake-up and stray field sensor was asserted low, but the system did not turn ON due to either U3 or U4 detecting this external magnetic field.

3.3.4 Current Consumption Results

表 3-4. Current Consumption Under Different Conditions

CONDITION	CURRENT FOR 5 V AT LDOIN	CURRENT FOR 18 V AT LDOIN	CURRENT FOR 3.3 V AT VCC
1: BJT optional circuit and LEDs removed (Everything else on the board is still enabled; current is measured at LDOIN)	6.578 μ A	6.946 μ A	–
2: Condition 1 + tamper sensor 1 disabled (Current is measured at LDOIN)	4.816 μ A	5.229 μ A	–
3: Condition 2 + tamper sensor 2 disabled (Current is measured at LDOIN)	3.112 μ A	3.427 μ A	–
4: Condition 3 + Stray field sensor disabled (Current is measured at LDOIN)	3.076 μ A	3.459 μ A	–
5: Condition 3 + LDO disabled (Wake-up Hall sensor, load switch, 4-channel NAND gate, and 1-channel NAND gate are still enabled; current measured at VCC)	–	–	1.67 μ A

Based on the desired level of protection against external magnetic fields and the system current consumption requirements, select which tamper and stray field sensors should be enabled. See [Section 2.3.2](#) for additional optimizations that can be done to reduce system current consumption.

4 Design and Documentation Support

4.1 Design Files

4.1.1 Schematics

To download the schematics, see the design files at [TIDA-060032](#).

4.1.2 BOM

To download the bill of materials (BOM), see the design files at [TIDA-060032](#).

4.2 Tools and Software

Tools

[HALL-TRIGGER-EVM](#) Order link to TIDA-060032 Hardware (also referred to as HALL-TRIGGER-EVM)

4.3 Documentation Support

1. Texas Instruments, [DRV5056 Unipolar Ratiometric Linear Hall Effect Sensor](#) data sheet
2. Texas Instruments, [DRV5032 Ultra-Low-Power Digital-Switch Hall Effect Sensor](#) data sheet
3. Texas Instruments, [TPS709 150-mA, 30-V, 1- \$\mu\$ A \$I_Q\$ Voltage Regulators With Enable](#) data sheet
4. Texas Instruments, [TPS22917x 1 V–5.5-V, 2-A, 80-m \$\Omega\$ Ultra-Low Leakage Load Switch](#) data sheet
5. Texas Instruments, [SN74HCS00 Quadruple 2-Input NAND Gates with Schmitt-Trigger Inputs](#) data sheet
6. Texas Instruments, [SN74AUP1G00 Low-Power Single 2-Input Positive-NAND Gate](#) data sheet
7. Texas Instruments, [TLV906xS 10-MHz, RRIO, CMOS Operational Amplifiers for Cost-Sensitive Systems](#) data sheet
8. Texas Instruments, TI Precision Labs - [Introduction to head-on applications](#) video

4.4 サポート・リソース

[TI E2E™ サポート・フォーラム](#)は、エンジニアが検証済みの回答と設計に関するヒントをエキスパートから迅速かつ直接得ることができる場所です。既存の回答を検索したり、独自の質問をしたりすることで、設計に必要な支援を迅速に得ることができます。

リンクされているコンテンツは、該当する貢献者により、現状のまま提供されるものです。これらは TI の仕様を構成するものではなく、必ずしも TI の見解を反映したものではありません。TI の[使用条件](#)を参照してください。

4.5 Trademarks

TI E2E™ are trademarks of Texas Instruments.
すべての商標は、それぞれの所有者に帰属します。

重要なお知らせと免責事項

TI は、技術データと信頼性データ(データシートを含みます)、設計リソース(リファレンス・デザインを含みます)、アプリケーションや設計に関する各種アドバイス、Web ツール、安全性情報、その他のリソースを、欠陥が存在する可能性のある「現状のまま」提供しており、商品性および特定目的に対する適合性の黙示保証、第三者の知的財産権の非侵害保証を含むいかなる保証も、明示的または黙示的にかかわらず拒否します。

これらのリソースは、TI 製品を使用する設計の経験を積んだ開発者への提供を意図したものです。(1) お客様のアプリケーションに適した TI 製品の選定、(2) お客様のアプリケーションの設計、検証、試験、(3) お客様のアプリケーションに該当する各種規格や、その他のあらゆる安全性、セキュリティ、規制、または他の要件への確実な適合に関する責任を、お客様のみが単独で負うものとします。

上記の各種リソースは、予告なく変更される可能性があります。これらのリソースは、リソースで説明されている TI 製品を使用するアプリケーションの開発の目的でのみ、TI はその使用をお客様に許諾します。これらのリソースに関して、他の目的で複製することや掲載することは禁止されています。TI や第三者の知的財産権のライセンスが付与されている訳ではありません。お客様は、これらのリソースを自身で使用した結果発生するあらゆる申し立て、損害、費用、損失、責任について、TI およびその代理人を完全に補償するものとし、TI は一切の責任を拒否します。

TI の製品は、[TI の販売条件](#)、または [ti.com](https://www.ti.com) やかかる TI 製品の関連資料などのいずれかを通じて提供する適用可能な条項の下で提供されています。TI がこれらのリソースを提供することは、適用される TI の保証または他の保証の放棄の拡大や変更を意味するものではありません。

お客様がいかなる追加条項または代替条項を提案した場合でも、TI はそれらに異議を唱え、拒否します。

郵送先住所 : Texas Instruments, Post Office Box 655303, Dallas, Texas 75265

Copyright © 2022, Texas Instruments Incorporated